Chapter 2

The IRAS Shell in Vela

2.1 Introduction

The IRAS Vela Shell is a ring-like structure seen in the region $l^{II} = 245°$ to $275°$, extending upto $b^{II} = -15°$. It was discovered in the course of a study of the interstellar medium in the Puppis-Vela region by M. Sahu (1992). The Shell was clearly seen in the IRAS (Infrared Astronomical Satellite) Sky Survey Atlas (ISSA) in the 25, 60 and 100 micron maps. The far IR emission indicates the presence of dust, and associated gas. It is seen projected against the Gum Nebula as a region of enhanced Ha emission in the southern part of the Nebula. The Gum Nebula itself is an extended, faint structure $\sim$ 36" in diameter and was tliscovered from a mosaic of long exposure Ha and NII emission maps by Colin Gum (1952). The case for identifying the Shell as a structure separate from the Gum Nebula primarily rests on two facts.

1. The rest of the Gum Nebula does not appear in the ISSA maps.
2. The Shell region appears to have kinematics different from the rest of the Gum Nebula.

The kinematics of the ionized gas in the Shell have been derived from the velocities of the emission line features of NII for several points within the Shell and comparison with other regions of the Gum Nebula. Two points near the center of the Shell show a double peaked structure indicating an expanding shell (the velocity of expansion being $\sim 10 \pm 2$ km s^{-1}). This is not the case for the rest of the Nebula. The ionized gas clearly has different velocity behaviour inside the Shell as compared to the rest of the Nebula. The Shell roughly envelopes the association of OB stars seen in the region (discovered by Brandt *et* al.1971) called the Vela OB2 association. Two of the brightest stars known, ζ Puppis (spectral

type O4If) and γ^2 Velorum, a Wolf-Rayet binary (O8.5III+WC8, van der Hucht *et al.,* 1997) are also seen in the vicinity of the Shell. Based on the symmetric location of the Shell with respect to Vela OB2, Sahu argued that this group of stars is associated with the Shell. The distance to the Vela OB2 association is estimated to be $\sim$ 450 pc (Sahu 1992) and this has been taken as the distance to the Shell as well.

Morphologically, the "dark clouds" (condensations of molecular gas and dust seen as patches of obscuration in optical photographs) and Cometary Globules present in the region appear to be part of the Shell. The Cometary Globules are dark clouds which show a head-tail structure (Hawarden and Brandt, 1976; Sandqvist, 1976; Zealey *et al.,* 1983; Reipurth, 1983). In a detailed study of the ^{12}CO emission from these globules Sridharan (1992) concluded that the Cometary Globules are expanding about a common center with a velocity of $\sim$ 12 km s^{-1}. If the Cometary Globules are associated with the Shell (as indicated by their distribution around the Shell), then this strengthens the claim for the expansion of the Shell. The tails of the Cometary Globules are seen to point away from a central region. Sridharan has determined the location of this morphological center, which is roughly centered on the Shell (see Fig 2.1).

The IRAS Point Source Catalogue (IPSC) also reveals a ring-like structure. The ring is especially well defined if one selects sources which are likely to be Young Stellar Objects (YSOs) typically characterised by their far infrared excess. This points to enhanced star formation in the Shell. Fig 2.2 shows the IRAS Vela Shell as seen in the IPSC, for sources satisfying certain criteria which are explained in section 2.3. *In the rest of this chapter we shall be concerned with this Shell as delineated by Young Stellar Object candidates.* This is slightly offset in position from the ISSA shell. In her study Sahu estimated the mass of the entire IRAS Vela Shell to be of the order of $\sim 10^6$ solar masses. The infrared flux from the IRAS Sky Survey Atlas maps was used to estimate the dust mass, and a dust to gas ratio of 100 was used to arrive at the gas mass. An estimate of the energy output from the Vela OB2 association in the form of supernovae, stellar wind and radiation led Sahu to suggest that the IRAS Vela Shell could be the remnant of a Giant Molecular Cloud sorrounding the Vela OB2 association.

In this chapter, we report our observations to look for molecular gas associated with the IRAS Vela Shell and also examine its kinematics . A broader scope of the enquiry would be to ascertain the quantity and kinematics of the gas in atomic, ionized and molecular form. As mentioned before, the only indicator so far of

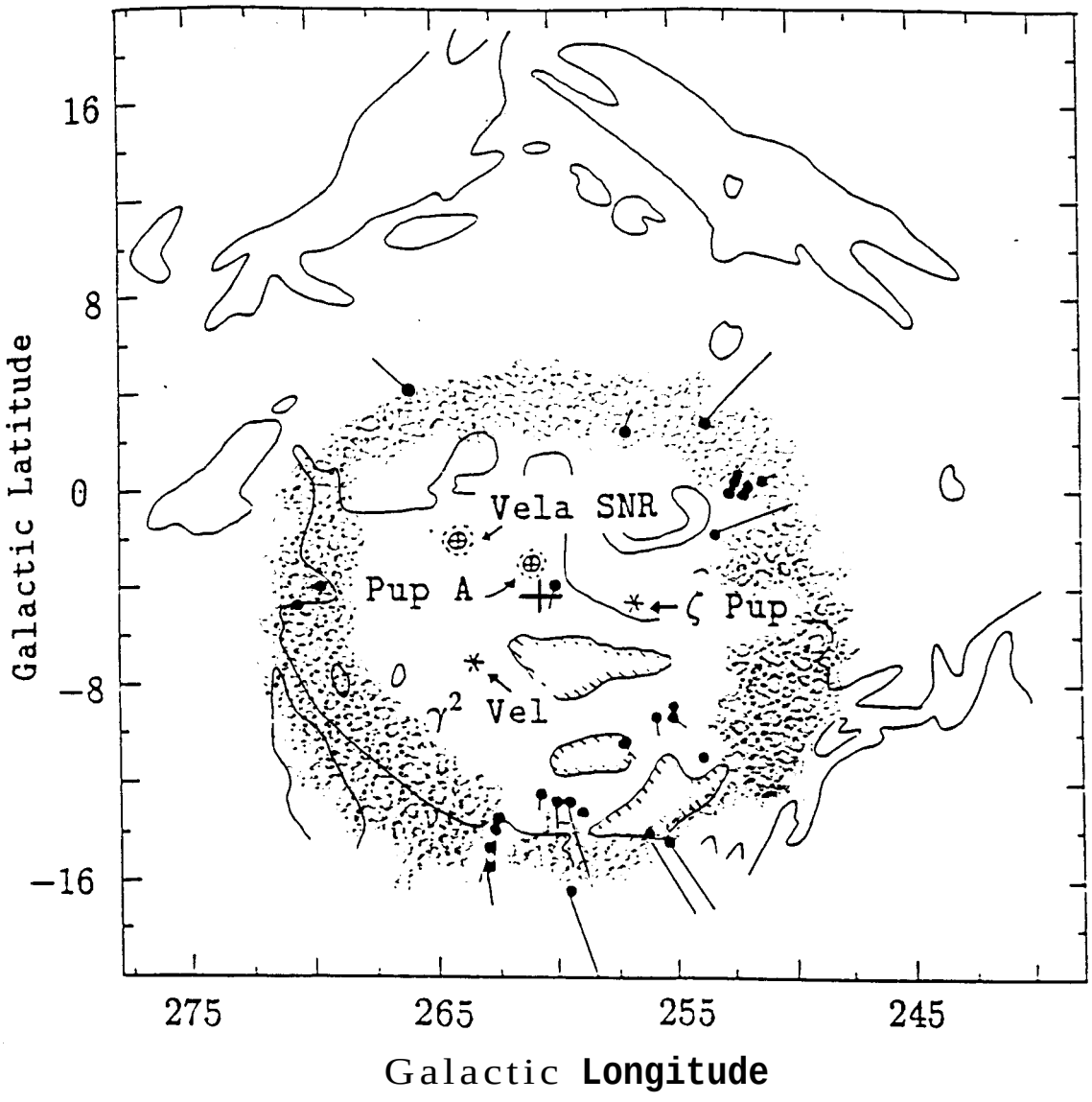

Figure 2.1: Overall picture of the Gum-Vela region showing the Hα emission as solid lines, the Cometary Globules as filled circles with tails (scaled up 10 times for clarity), and other important objects in the region. The morphological centre of the system of Cometary Globules is indicated by a + sign. The molecular Shell that we have detected, and which is the subject of this chapter is depicted as a shaded shell. Adapted from Sridharan (1992).

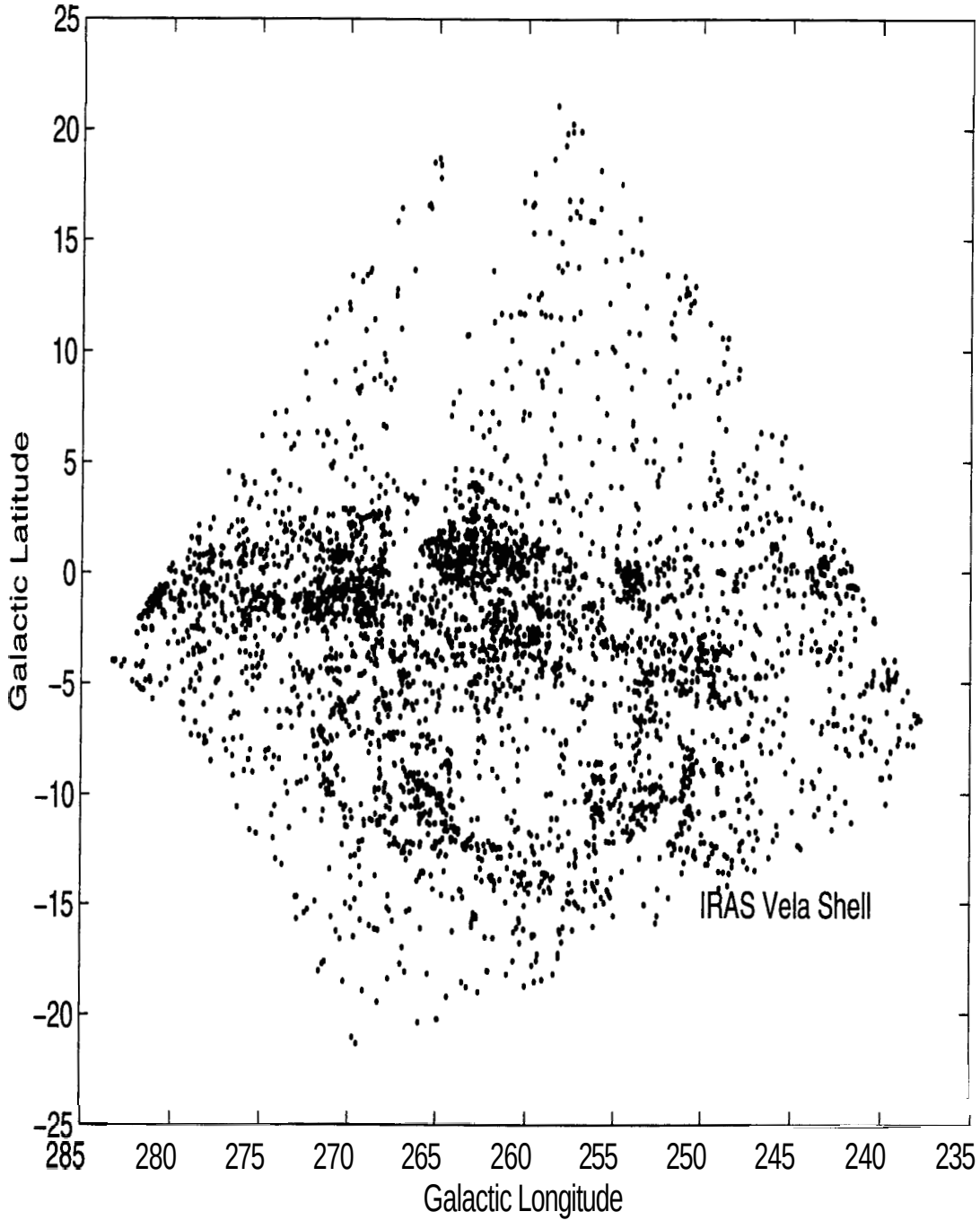

Figure 2.2: IRAS Point Sources between $l = 240°$ and $l = 280°$. These sources satisfy the criteria for Young Stellar Object candidates listed in the text. The IRAS Vela Shell is noticeable below the Galactic plane.

the motion of the molecular gas associated with the Shell is the kinematics of the Cometary Globules themselves. These are only a small subset of the large number of "dark clouds" which are seen in this region and which also seem to be associated with the Shell through their morphology. Moreover, the Cometary Globules are a special population as revealed by their peculiar morphology. Hence a more general study of the molecular gas in the region seemed warranted. To this end we undertook millimeter wave observations of the Shell in the rotational transition $J = 1 \rightarrow 0$ of the ^{12}CO molecule at 115.271 GHz. We looked for detections towards a randomly selected sample of IPSC sources delineating the Shell.

The dark clouds in the region also seem to roughly define a shell as seen in the optical extinction maps of Feitzinger and Stiiwe (1984) reproduced in Fig **2.3.** If they are indeed associated with the Shell, they form a major part of the molecular content. We examine the kinematics of the dark clouds using ^{12}CO velocities in order to study their inter-relation to the Shell and the Cometary Globules. The emerging picture of the nature of the Shell is discussed in detail.

2.2 Millimetre wave astronomy with the ^{12}CO molecule

Molecular clouds represent the cool dense component of the interstellar medium with densities of the order of $10^3 cm^{-3}$ and temperatures in the range of a few degrees Kelvin. The most abundant molecule in these clouds is, of course, hydrogen. However the H_2 molecule is not easily observed. It lacks a permanent dipole moment and does not radiate in its lower rotational transitions. The lowest rotational transition $(J = 2 + 0)$ has an energy corresponding to a temperature of $\blacksquare$ 509 K, which is much higher than the typical kinetic temperature in the clouds. The vibrational-rotational quadrupole transitions of the H_2 molecule fall in the IR, requiring temperatures of $\sim$ 1000 K. These lines can only be used to study shock excited regions. The UV absorption line of H_2 is obviously useful only towards selected lines of sight. Thus direct observations of H_2 in cold environments is not possible. Carbon monoxide is the most widely observed molecule in interstellar gas. It is used to probe clouds in our Galaxy as well as external galaxies. It is also believed to be the second most abundant molecule and is used as a tracer for H_2. It has a permanent dipole moment leading to conveniently observable radio lines. The lowest rotational transition $J = 1 \rightarrow 0$ at 115 GHz corresponds to a temperature of 5.5 K. It also has a relatively small electric dipole moment of

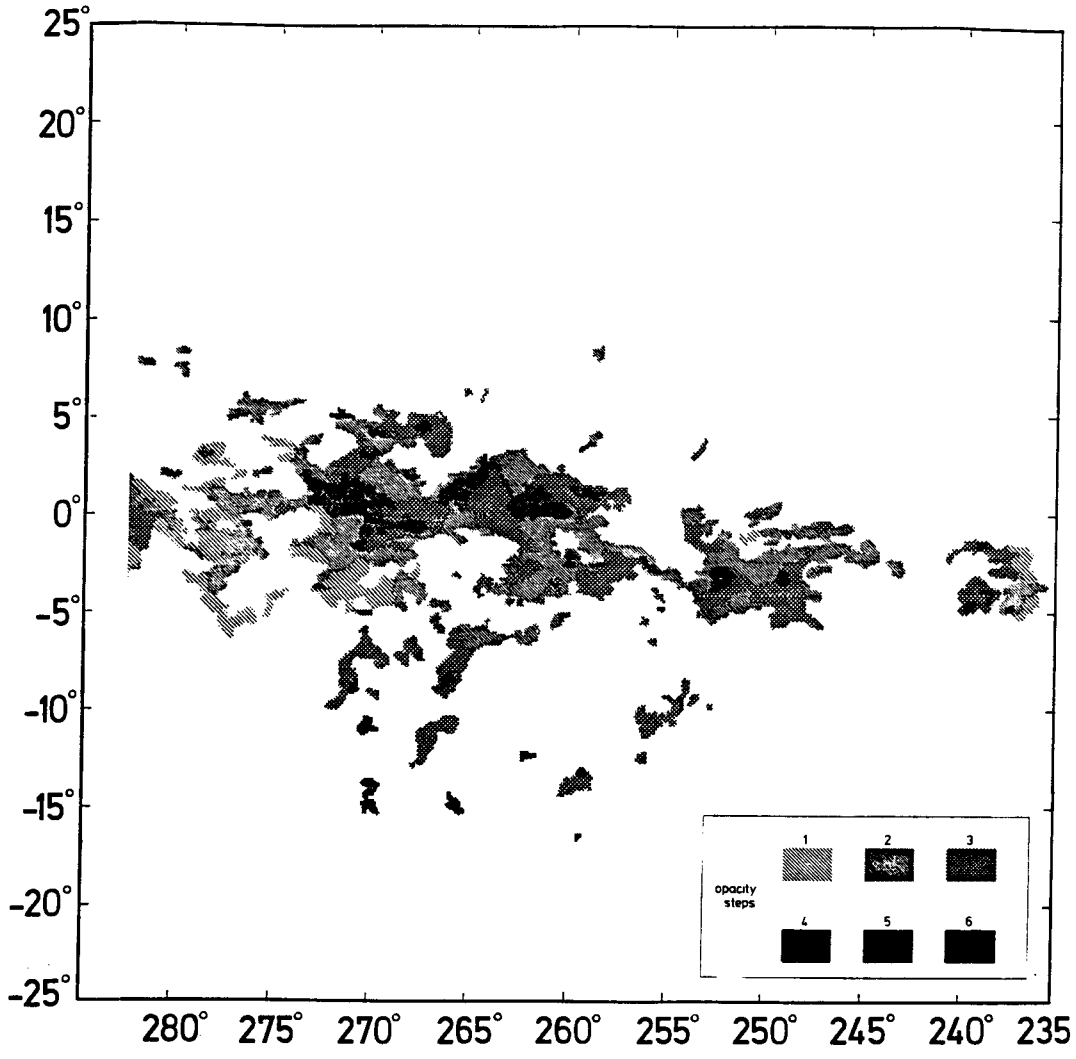

Figure **2.3:** A part of the optical extinction map made from ESO/SERC southern sky survey by Feitzinger and Stüwe(1984). The map shows the dark nebulae (defined as having an area greater than 0.01 sqdeg) in the region of the molecular Shell. The ring-like structure of these nebulae is evident. The opacity classes (indicative of the degree of absorption) is indicated below the map.

$\sim$ 0.1 D and is easily excited into emission above the background even at modest interstellar densities. CO also has several isotopic varieties and the less abundant ^{13}CO is used to probe deeper into the molecular cloud cores without encountering optical depth problems. An additional advantage in using CO is that almost all of its lower rotational transitions lie within the usable atmospheric window for ground based telescopes.

2.3 Source selection

In order to increase our chances of detecting molecular material we chose a sample of the IPSC sources which satisfied certain criteria. It has been noted that the definition of the Shell is improved if one selects sources which are likely to be Young Stellar Objects (YSOs) which point to star formation activity in the shell. The Shell is quite prominent in maps of IPSC sources which satisfy "Classifier III" criteria, a method used by Prusti (1992) to pick out YSO candidates in the IPSC. However "Classifier III" uses, in addition to colour and statistical criteria, certain "crowding" properties which would enhance the Shell. Using such a filter would bias the distribution of sources selected for the survey and it would be difficult to determine if the sources are distributed in a volume or shell. We have therefore restricted ourselves to selecting sources which satisfy YSO candidate criteria used by Sridharan (1992), which are from Emerson (1987) and Parker (1988). These are as listed below.

1. Detection at 25μm and 60μm with $[60 - 25] > 0$.
2. $[25 - 12] > 0$, if also detected at 12μm.
3. Detection only at 60μm.
4. Detection at 60μm and 100μm only with $[100\text{-}60] > 0.6$
5. $[100 - 25] > 0$

Here [25 - 12], for example, refers to the 25 to 12 micron color $= \log[S_{25}/S_{12}]$, S_{25} being the IPSC flux density in Jansky at 25μm wavelength.

We used this filter on the IPSC sources in the RA range 7 hrs to 9 hrs, which covers the Shell. Fig 2.2 shows the distribution of these sources in Galactic coordinates clearly revealing the IRAS Vela Shell. Out of the $\sim$ 3750 sources which met the criteria, we were able to observe $\sim$ 100 given our limited observing

season. The coverage encompasses the Shell but is not uniform. We also observed several regions within the Shell which did not have IPSC sources.

2.4 Observations

The observations were done with the 10.4m radio telescope at the Raman Research Institute. Details of the telescope and the subsystems have been described in detail by Patel (1990). The telescope has an altitude-azimuth mount with the receiver at the Nasmyth focus. The receiver is a 20 K cooled Schottky mixer type with 1.5 GHz IF. The backend used was a hybrid type correlation spectrometer configured for a bandwidth of 80MHz with 800 channels giving a resolution of $\approx$ 100 KHz, when using both polarizations. This corresponds to a velocity resolution of 0.26 km s^{-1}.

The observations were done in the frequency switched mode. This has the advantage that no time is spent looking at source-free regions. Moreover, since we could be observing extended sources, the off source regions are not well defined for beam switching schemes. During frequency switching the spectral line from the source is received in different parts of the receiver band during alternate switching periods. This would mean that the receiver characteristics change slightly between the ON and OFF spectra due to retuning. This introduces curvature in the baseline after subtraction. However, unless one is expecting low level wide features baseline curvature is not a serious drawback. A frequency offset of 15.25 MHz was chosen between ON and OFF spectra since that is the period of the observed baseline ripple. With this scheme only a polynomial fit was required to remove any residual baseline curvature. The switching rate was 2 Hz. Calibration was done using an ambient temperature chopper at intervals of several minutes. Pointing error, as obtained from observing Jupiter, was within 20". The frequency stability of the correlator was checked by observing the head of the Cometary Globule CG 1 each day. The rms of this distribution was 0.3 km s^{-1} and will be the error on velocities quoted in this chapter. Comparison of the measured velocities of the heads of CG 1, as well as several other Cometary Globules, with those measured by Sridharan (1992) shows good agreement.

The observations were carried out during the period March to April 1996. The optical depth at 115.271 GHz measured at zenith was rather poor during this period and ranged from 0.2 to 0.5. Each run consisted of typically ten minutes of integration in the direction of the selected IPSC source. The spectra in the

vertical and horizontal polarizations were then averaged after removing baseline curvature. The effective integration time was therefore typically of the order of 20 minutes. The rms noise over such integration periods was of the order of 0.2 K. A typical spectrum after removal of a fourth order polynomial to correct baseline curvature is shown in Fig 2.4. Data reduction was done using the UNIPOPS package.

2.5 Basic Calibration

The temperature scale obtained by the reduction procedure described in the previous section is usually denoted by T_A^*. This quantity is telescope dependent. However, in this experiment we are interested only in the detections and the velocities rather than in the absolute temperatures. We therefore do not correct them further and all temperatures quoted for our detections are T_A^*. The basic calibration is as follows.

An observation consists of an ON and OFF measurement, followed by an AMB and OFF measurement. In our case, the ON and OFF correspond to two different frequencies (frequency switching) and AMB is done with an ambient temperature absorber introduced in front of the receiver. If the corresponding voltages are V_{ON}, V_{OFF} and V_{AMB} and the system gain (including atmosphere) is G_s and G_i in the signal and image bands, we have, for a double side band system (DSB),

$$V_{ON} = G_s T_{sys,s} + G_i T_{sys,i} + G_s T_{source} \quad (2.1)$$

$$V_{OFF} = G_s T_{sys,s} + G_i T_{sys,i} \quad (2.2)$$

$$V_{AMB} = G_s T_{sys,s} + G_i T_{sys,i} + (G_s + G_i) T_{amb} \quad (2.3)$$

from which we get

$$T_{source} = T_{AMB}(1 + \frac{G_i}{G_s}\frac{V_{ON} - V_{OFF}}{V_{AMB} - V_{OFF}}) \quad (2.4)$$

T_{source} is normally referred to as T_A^*, the antenna temperature after correction for all telescope losses occuring at ambient temperature.

2.6 Results

We detected emission from ^{12}CO towards 42 of the $\sim$ 100 IPSC sources that we observed. Table 2.1 lists the measured antenna temperatures and LSR velocities

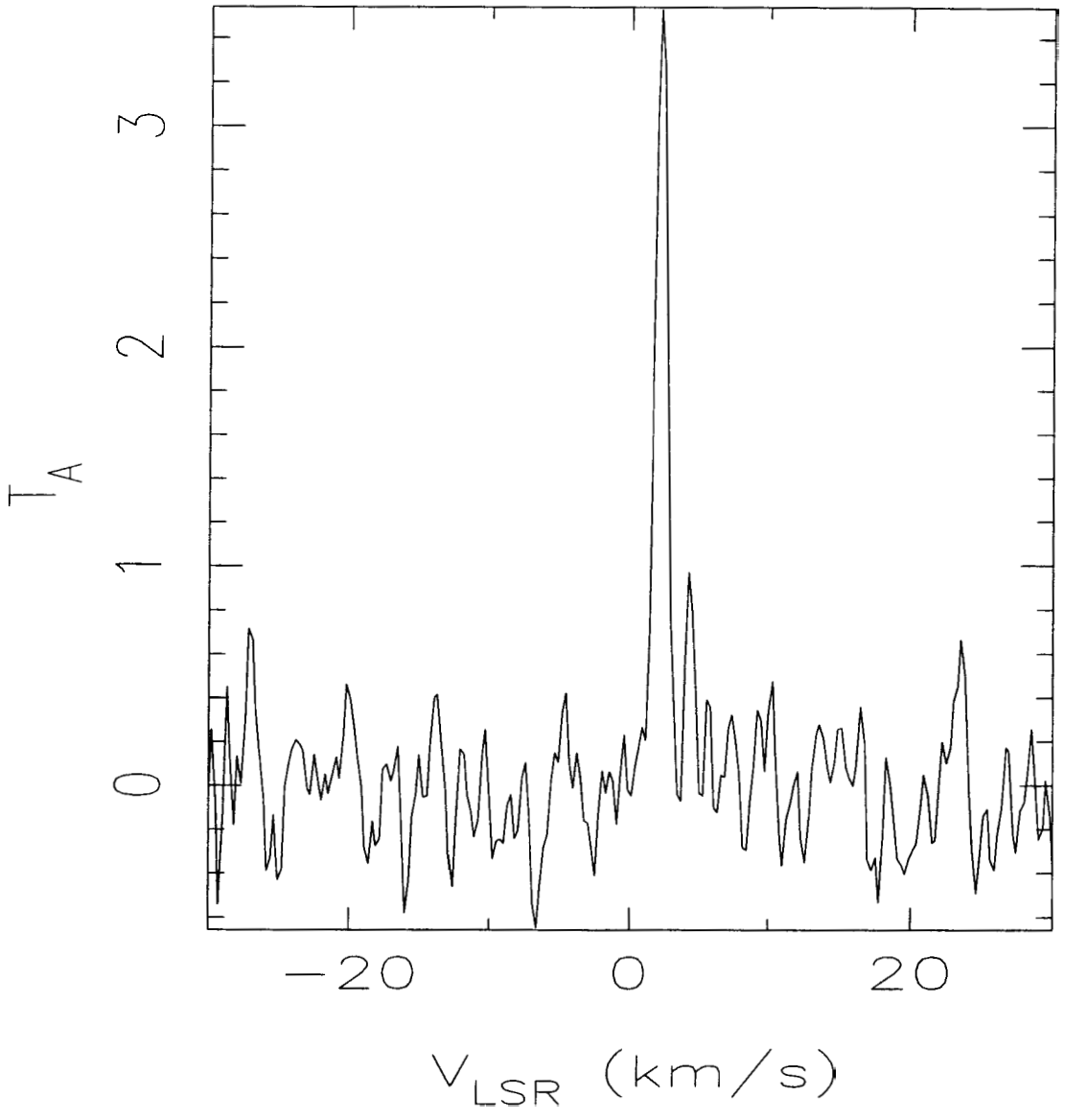

Figure 2.4: A typical spectrum showing ^{12}CO emission (J = 1→ 0 transition, λ = 2.6mm, ν_0 = 115.271 GHz) after removal of a polynomial fit to the baseline. The spectrum was obtained towards the IRAS point source IR 56549 in the Shell. The vertical axis shows T_A * (calibrated antenna temperature) in K. The effective integration time was $\sim$ 20 minutes.

Source	V_{lsr}	$T_A{}^*$	T_{rms}	Source	V_{lsr}	$T_a{}^*$	T_{rms}
	km s^{-1}	K	K		km s^{-1}	K	K
51704	-1.2	0.6	0.12	61322	8.4	2.2	0.22
52594	-2.5	0.9	0.18	61322	13.2	1.5	0.22
53668	-0.5	0.5	0.13	61351	8.1	1.2	0.26
53829	-3.4	0.4	0.13	61428	7.7	3.0	0.14
54473	-1.2	0.8	0.18	61837	3.0	4.6	0.20
54599	-2.2	3.3	0.23	62100	9.9	7.7	0.12
54769	-3.1	1.7	0.13	62578	14.9	0.6	0.15
55878	-5.0	4.5	0.13	62717	3.9	3.3	0.21
55884	4.4	2.8	0.18	62841	-1.0	2.1	0.45
55925	5.5	0.9	0.24	62847	5.4	0.7	0.17
55932	21.5	0.8	0.14	63338	14.4	0.7	0.17
56549	2.2	3.6	0.27	63338	9.4	1.9	0.17
56831	-1.5	1.2	0.17	63927	4.6	1.4	0.20
57035	16.4	1.5	0.16	64029	8.8	3.7	0.16
57035	28.6	1.9	0.16	64154	14.1	1.4	0.16
57898	1.4	5.2	0.37	64388	0.9	2.2	0.14
58784	-8.2	1.1	0.18	64728	10.6	1.2	0.27
58793	8.6	0.3	0.12	64999	-4.0	1.1	0.25
58793	9.6	0.3	0.12	65728	7.0	2.4	0.27
59579	-7.5	0.9	0.24	65877	4.9	9.3	0.31
59584	5.7	0.8	0.18	66001	1.8	1.3	0.36
59891	-6.3	0.9	0.24	67910	6.0	3.3	0.30
60933	0.3	1.3	0.18	69185	3.5	2.0	0.30

Table 2.1: Summary of molecular detections toward IRAS Point Sources: Column 1 lists the IRAS Point Source catalogue number for the source. Columns 2 and 3 give the LSR velocity and the corrected antenna temperature (see section 2.5). Column 4 gives the rms noise level for each source. The **table is continued in Columns 5 to 8.**

found by fitting gaussians to the spectra. In cases where a source appears more than once, multiple features were detected at different velocities. Fig 2.5 shows the distribution of observed sources in galactic coordinates, with both detections as well as non-detections included. From Fig 2.5, the distribution of our detections also hints at a ring like geometry. We failed to detect molecular emission down to our sensitivity limits of ~ 0.6 K from a few *blank regions* that we selected within the Shell (these are not shown in the figure). As seen in the figure the points observed more than $\sim 2°$ above the Galactic plane also failed to yield detections. A gap is seen in the distribution of detections in the lower part of the Shell (the lower right hand side of the figure). Interestingly, this also happens to be a region where there are a number of Cometary Globules (we have not included any of the Cometary Globules in our list of detections). This seems to suggest that the region around the Cometary Globules have been cleared of molecular material, although a much more complete mapping would have to be undertaken to say this with a reasonable amount of confidence.

2.7 The Southern Dark Clouds

As briefly mentioned in the introduction, the dark clouds seen in the region of the Shell also seem to define a shell-like structure.

Recntly a general survey of all the dark clouds in the southern sky listed in the Catalogue of Dark Clouds (Hartley *et al.*, 1986) was done in the 115 GHz line of the ^{12}CO molecule (Otrupcek, Hartley and Wang Jing-Sheng, 1995) from the recently completed Mopra telescope, one of the antennae which make up the Autralia Telescope National facility. The survey was done in order to explore the association of molecular material with these clouds which were originally identified from optical surveys and study some of their global properties. *The survey happens to cover all the clouds in the vicinity of the Shell as well.* This fortuitous circumstance obviated the need for an extensive survey of the dark clouds in the region of the Shell using the Raman Institute 10.4 m telescope! From the spectra obtained in the Mopra survey which were kindly made available to us by Otrupcek, we identified those towards the region of the Shell. The SDCs from the Mopra catalogue in the vicinity of the Shell are shown in Fig 2.6 along with the IPSC sources towards which molecular material had been detected by us. It is evident that these dark clouds share the Shell morphology with a radius of $\sim 12.5°$.

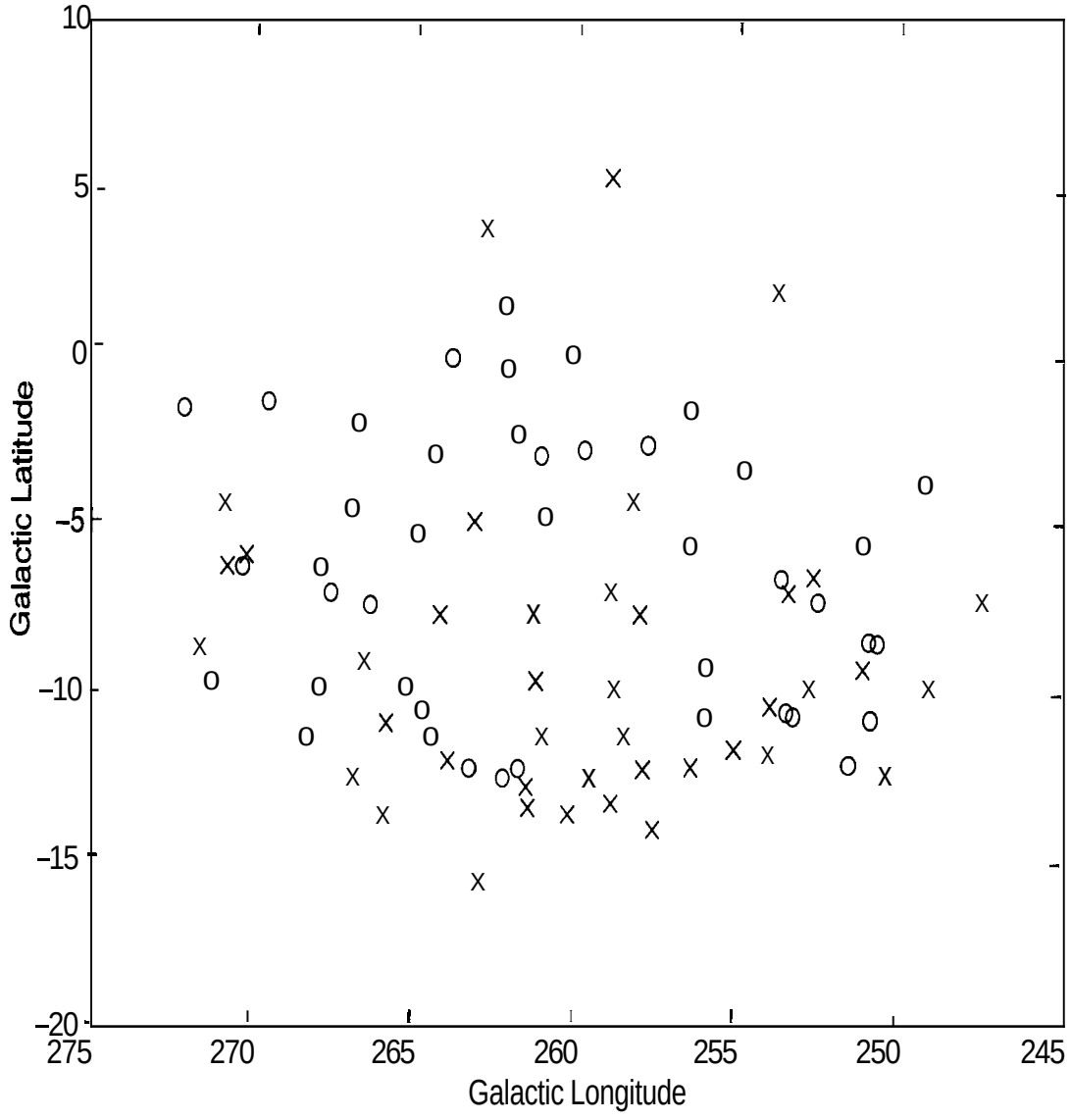

Figure **2.5:** Sources observed by us for CO emission are shown in Galactic coordinates. The circles denote detections and the crosses indicate non-detections. We have 42 detecions from $\sim$ 100 pointings. The sensitivity limit was $\sim$ 0.6 K.

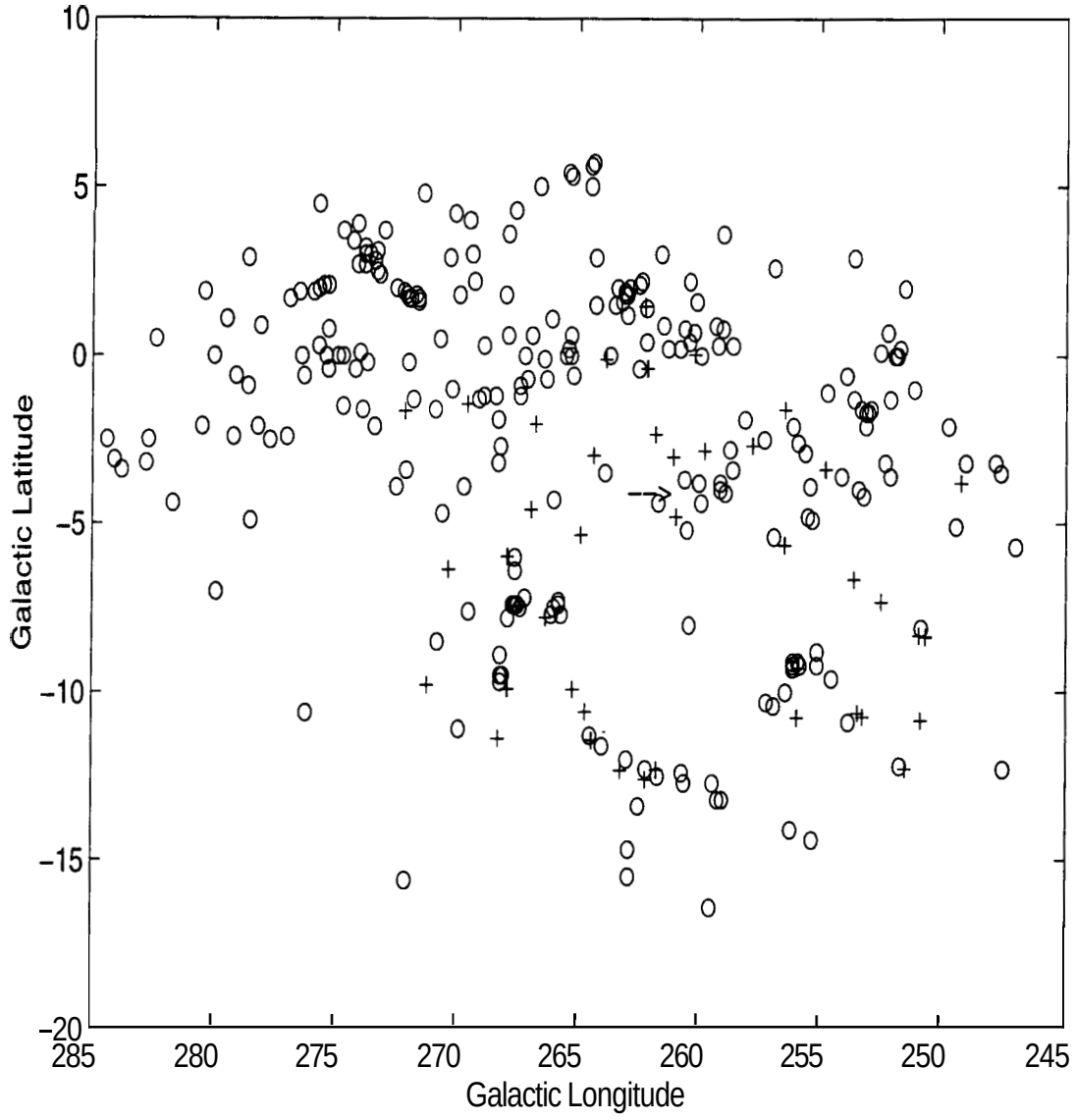

Figure 2.6: The figure shows the molecular detections towards IRAS point sources (plus signs), and the Southern Dark Clouds including Cometary Globules in the region of the IRAS Vela Shell shown as open circles. The arrow indicates the morphological center of the Cometary Globule system.

2.8 Kinematics

There have been earlier studies of the kinematics of the gas in the region. Sridharan (1992) had studied the kinematics of the Cometary Globules. From observations of the J = 1→0 transition of the ^{12}CO molecule, he concluded that the Cometary Globules were expanding from an apparent common center with an expansion velocity of $\sim$ 12 km s^{-1}.

Observations of this region in ionized gas have also been done (Sahu 1992, and references therein). These were carried out in the optical H a (6563Å), [NII] (6548Å, 6584Å) and [OIII] (5007 Å) emission lines. These observations covered the entire Gum Nebula, of which the Shell is only a part, and form an extension of various studies to determine the possible expansion of the Gum Nebula. There were about 4 to 5 pointings within the Shell. The double peaked profile of the [NII] line in the central region of the shell is consistent with an expansion velocity of $\sim$10$\pm$2 km s^{-1}. In Fig 2.7 we reproduce a schematic from Sahu showing the observed regions and the spectra of ionised gas. This agreement in the kinematics of the ionised gas and the molecular gas associated with the Cometary Globules led Sahu to conclude that the ionized gas as seen in H a emission is associated with the molecular gas seen in the dark clouds and Cometary Globules.

2.8.1 Expansion of the Shell of Infrared Point Sources

In this section we look at the radial velocities of the molecular material detected in the Shell, and see if they are consistent with an expansion from some common center. We have adopted the morphological center of the Cometary Globule system (marked in Fig 2.6) as the center of expansion for this study. Sridharan has identified this point, (l, b) = (260°,−4°), as the one towards which the maximum fraction of the Cometary Globules point to. In Fig 2.8, we show the location of this point with respect to the CG system. This point appears to us to be the logical choice for a common center for the Cometary Globules, SDCs, as well as the IPSC sources in which we have detected molecular gas. This seems reasonable since all the three populations are presumably associated in their spatial distribution. The angular separations of all objects are calculated with reference to this point which is marked in Fig 2.6. The maximum measured separation from the center for any of our detections is $\sim$ 12.5°.

If these objects are distributed in a shell and are expanding from a common center with a velocity v_{exp}, then the residual radial velocity v_{res} (after removing

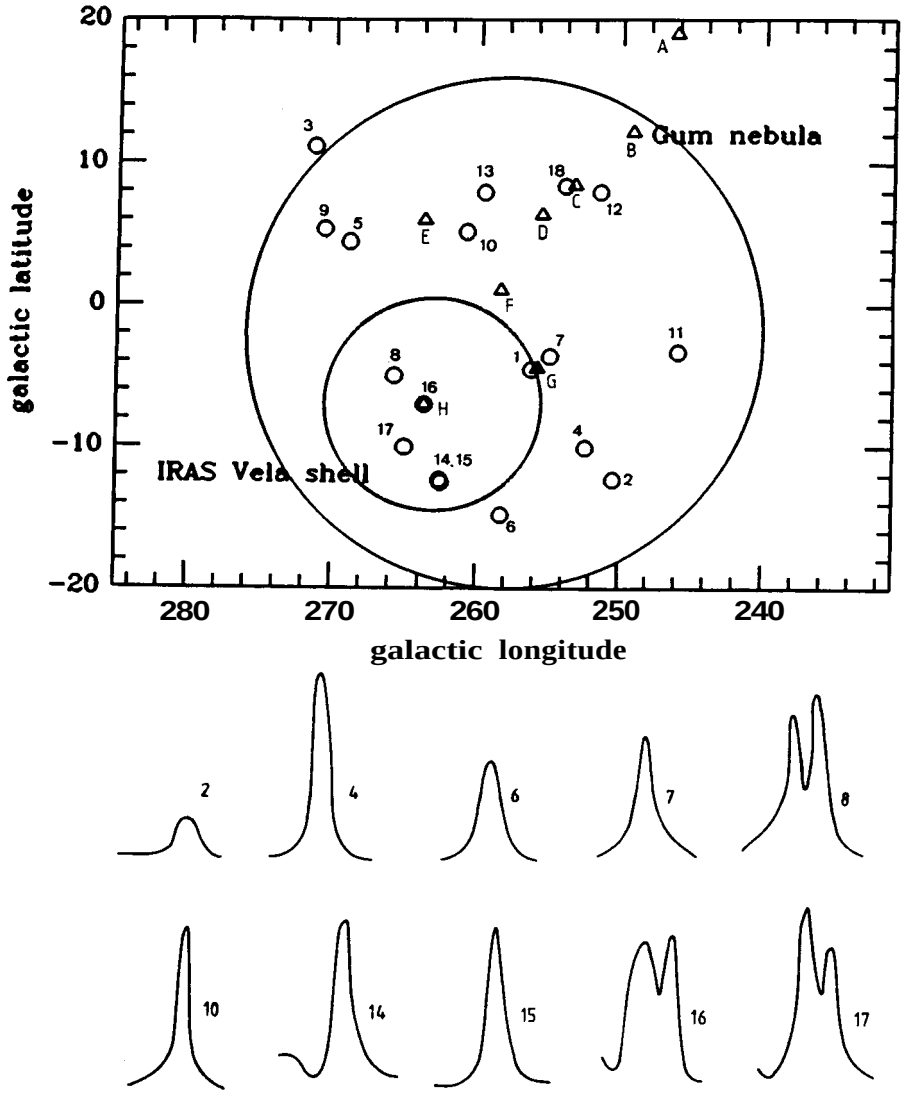

Figure 2.7: A schematic diagram of the Ha emission from the Gum Nebula and the IRAS Vela Shell (as sketched by Sahu 1992) is shown, along with the positions at which high resolution spectra of ionised gas were made by Sahu. The positions are indicated by small circles and labelled by numbers. The positions observed by Reynolds (1976a) are shown as small triangles. Plotted below are shapes of the NII λ6584Å profiles obtained at different positions. Note that only the central positions (nos. 8, 16 and 17) of the IRAS Vela Shell show a double peaked structure in the NII line. This is also supported by the observations of Reynolds (position H). This suggests an expansion of the ionised gas with a velocity of $\sim$ 10$\pm$ 2km s^{-1}. The figure is reproduced from Sahu (1992).

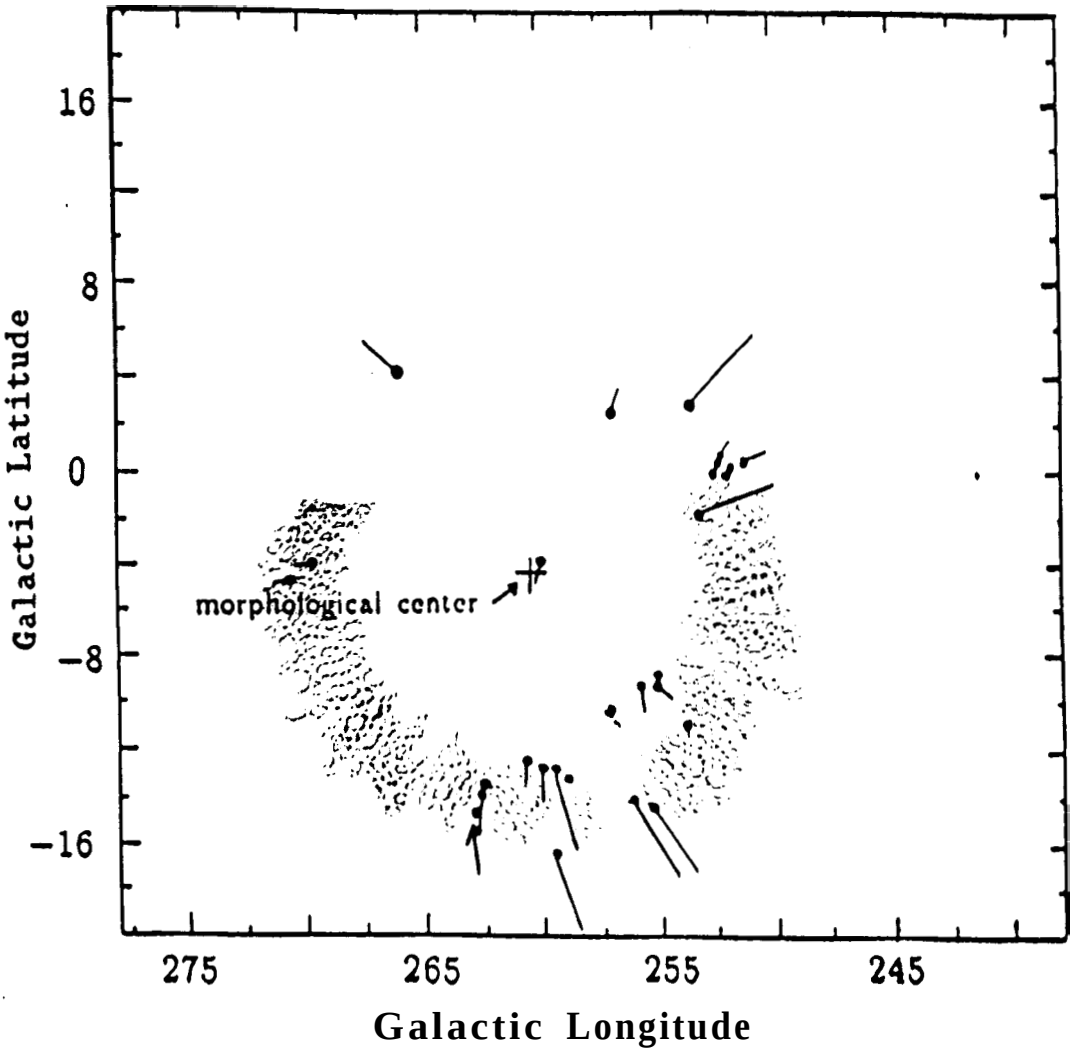

Figure 2.8: The morphological center of the Cometary Globule system and its location with respect to the Cometary Globules which are shown as dots with tails. The tails are exaggerated for clarity. The envelope of the inolecular Shell is shown. Adapted from Sridharan (1992).

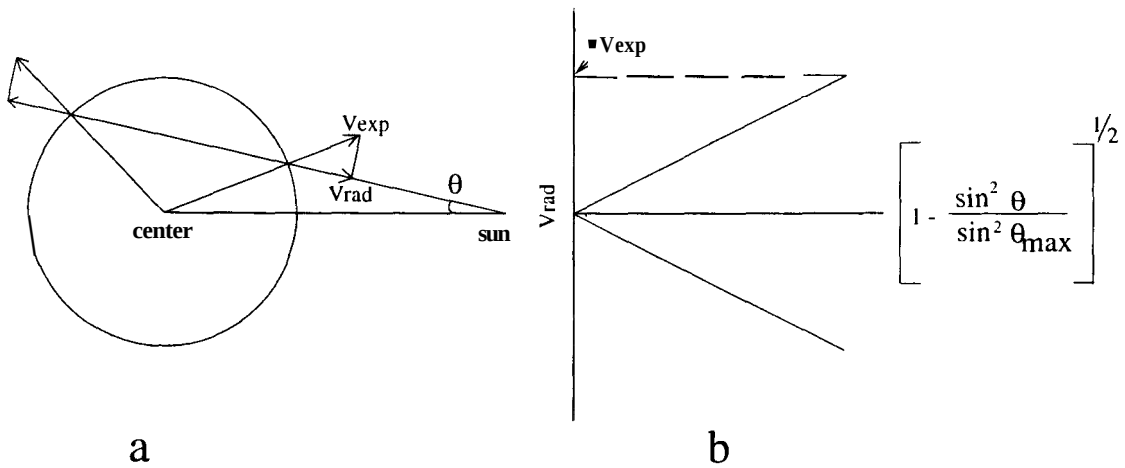

Figure 2.9: (a) A schematic for deriving expected radial velocities from an expanding shell. V_{exp} is the expansion velocity, V_{rad} is the radial component and Θ is the angular separation of any point on the shell from the center. (b) V_{rad} plotted against $(1-sin^2\theta/sin^2\theta_{max})^{1/2}$.

Galactic rotation component) will be related to v_{exp} through the formula

$$v_{res} = \pm v_{exp}(1 - \sin^2\theta/\sin^2\theta_{max})^{1/2}$$

where θ is the separation of the object from the center of expansion and θ_{max} is the maximum separation defining the shell as in Fig 2.9a. In a plot of v_{res} versus $(1 - \sin^2\theta/\sin^2\theta_{max})^{1/2}$, the points would then lie along two straight lines as shown in Fig 2.9b. **If the points are distributed in a volume rather than a shell, the points would tend to lie within the envelope defined by these two lines, provided the inner points are expanding slower than the outer points.**

We have removed from the measured LSR velocity of each detection the radial velocity component corresponding to the Galactic rotation velocity at the assumed distance to the center of the expansion. The radial component of Galactic rotation was determined from the formula

$$v_r = \mathrm{A}d \sin 2l \cos^2 \mathrm{b}$$

The heliocentric distance to the shell, d = 450pc, 1 = 260°, and b= −4°. This value for the distance is the accepted one for the Cometary Globules arrived at from distances to the early type stars including the Vela OB2 association seen

in the region (Wallerstein, Silk and Jenkins 1980; Brandt et *al.*1971), as well as from the distance to the young star seen in the head of the Cometary Globule CG1 (Brand et al., 1983). In section 2.10.3 we further comment on this distance estimate based on the new results from the Hipparcos satellite. We have assumed a value of 14.5 km $s^{-1}kpc^{-1}$ for Oort's constant A (Kerr and Lynden-Bell, 1986).

Fig 2.10 shows v_{res} against $(1 - \sin^2\theta/\sin^2\theta_{max})^{1/2}$. In this plot, only detections with $b < -4"$ have been included. Close to the Galactic plane there is increased chance of contamination from objects in the plane which are unrelated to the Shell. For example, the Vela Molecular Ridge is a region of enhanced molecular emission seen to lie in the proximity of the Shell, with a velocity range comparable to the velocities that one sees in the Shell (May et *al.*, 1988; Murphy and May, 1991). However, the distance to the Vela Molecular Ridge is estimated to be about 1 kpc, well beyond the Shell. We have restricted ourselves to $b < -4"$ to reduce the possibility of such contamination.

Fig 2.10 is consistent with a scenario of expanding molecular material occupying a filled volume. The signature of expansion is that the points shown in Fig 2.10 seem to be confined to a cone similar to the one shown schematically in Fig 2.9. There is an envelope to the measured velocities which increases as one approaches the center of the Shell (abscissa = 1). The dotted lines in Fig 2.10b show an envelope corresponding to an expansion velocity of 13 km s^{-1} and an offset of -3 km s^{-1} from zero. The offset would signify a velocity for the Shell as a whole. An envelope which would include most of the points could have a range of offsets and expansion velocities. The envelope shown in Fig 2.10b seems a better "fit" than the one in Fig 2.10a, even by visual inspection. The values of expansion velocity and offset shown in Fig 2.10b were arrived at as described in the next section. The density of points is low at low values of the abscissa. These are detections at the edge of the observed Shell and are sparse because of sampling effects. The sparseness of points at the left of the plot may tend to enhance the effect of velocities increasing to the right and thus mimic expansion.

2.8.2 Expansion of the Shell of molecular gas

As mentioned earlier, the Southern Dark Clouds also seem to be distributed as a Shell, just as the IRAS point sources. This association would be strengthened and the suspected expansion confirmed if the Southern Dark Clouds also show a similar kinematic behaviour. The Cometary Globule system is already known to show expansion although they are very few in number. Fig 2.11 shows a

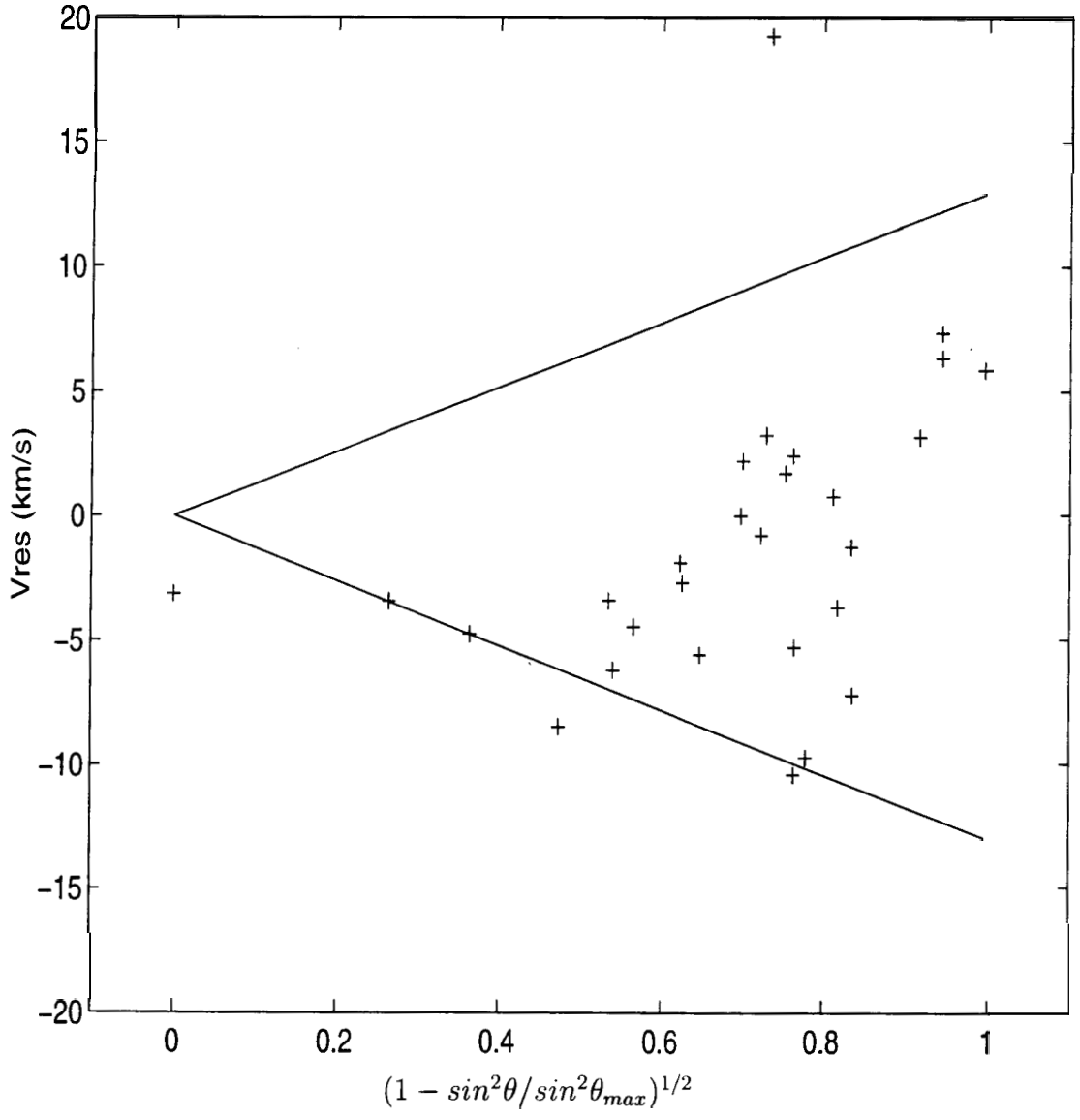

Figure 2.10: (a) The residual radial velocity after removing the Galactic rotation component plotted against the "expansion parameter" *i.e.*, $(1 - sin^2\theta/sin^2\theta_{max})^{1/2}$. θ is the angular separation of the source from the assumed center of expansion. If the objects form an expanding shell, the points will lie on the two straight lines (the "envelope") shown. If they are distributed in a volume, the points tend to lie within the envelope, as is the case here. The envelope shown is for an expansion velocity of 13 km s^{-1} with an offset of 0 km s^{-1}.

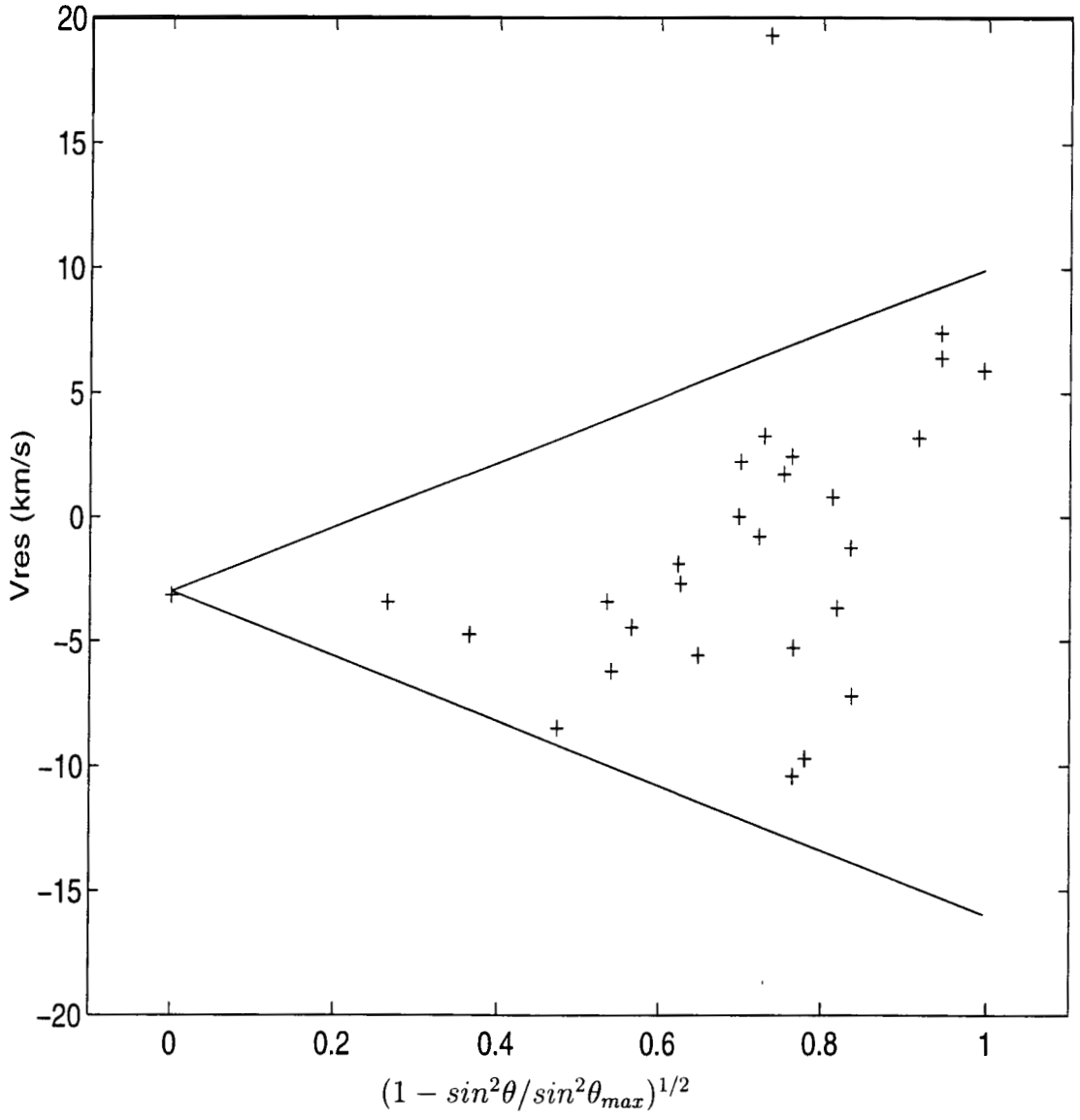

Figure 2.10: **(b)** The residual radial velocity after removing the Galactic rotation component plotted against the "expansion parameter" *i.e.*, $(1 - sin^2\theta/sin^2\theta_{max})^{1/2}$. All parameters are the same as in Fig 2.10a, except that the offset is -3 km s^{-1}. The points are better "fit" by this envelope than the one in Fig 2.10a

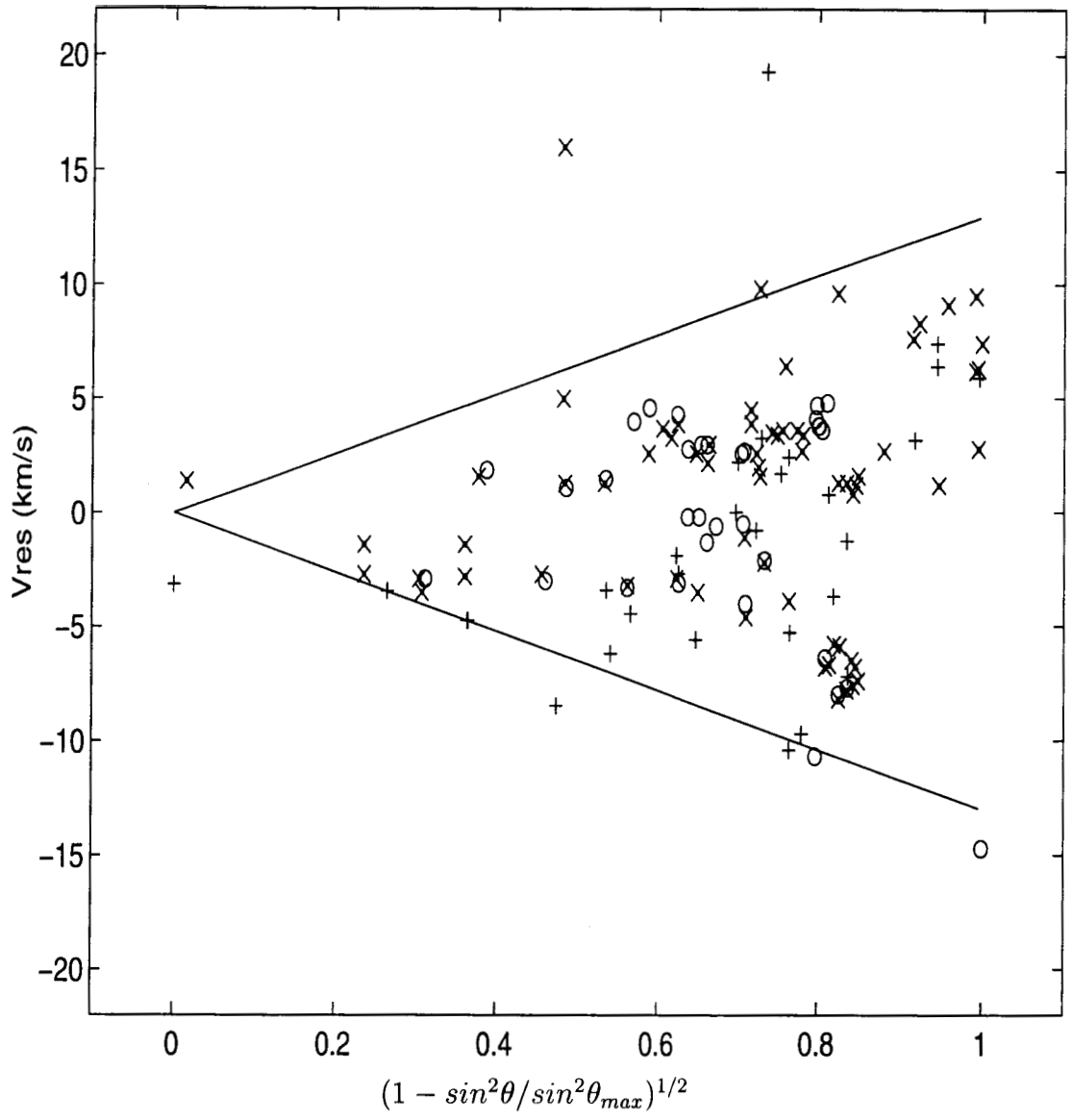

Figure 2.11: (a) The residual velocity plotted against $(1-sin^2\theta/sin^2\theta_{max})^{1/2}$ for all objects. The crosses denote SDCs, the open circles are Cometary Globules and the plus signs show molecular detections towards IPSC sources. The "expansion envelope" is for an expansion velocity of 13 km $s^{-1}$and offset of 0 km s^{-1}.

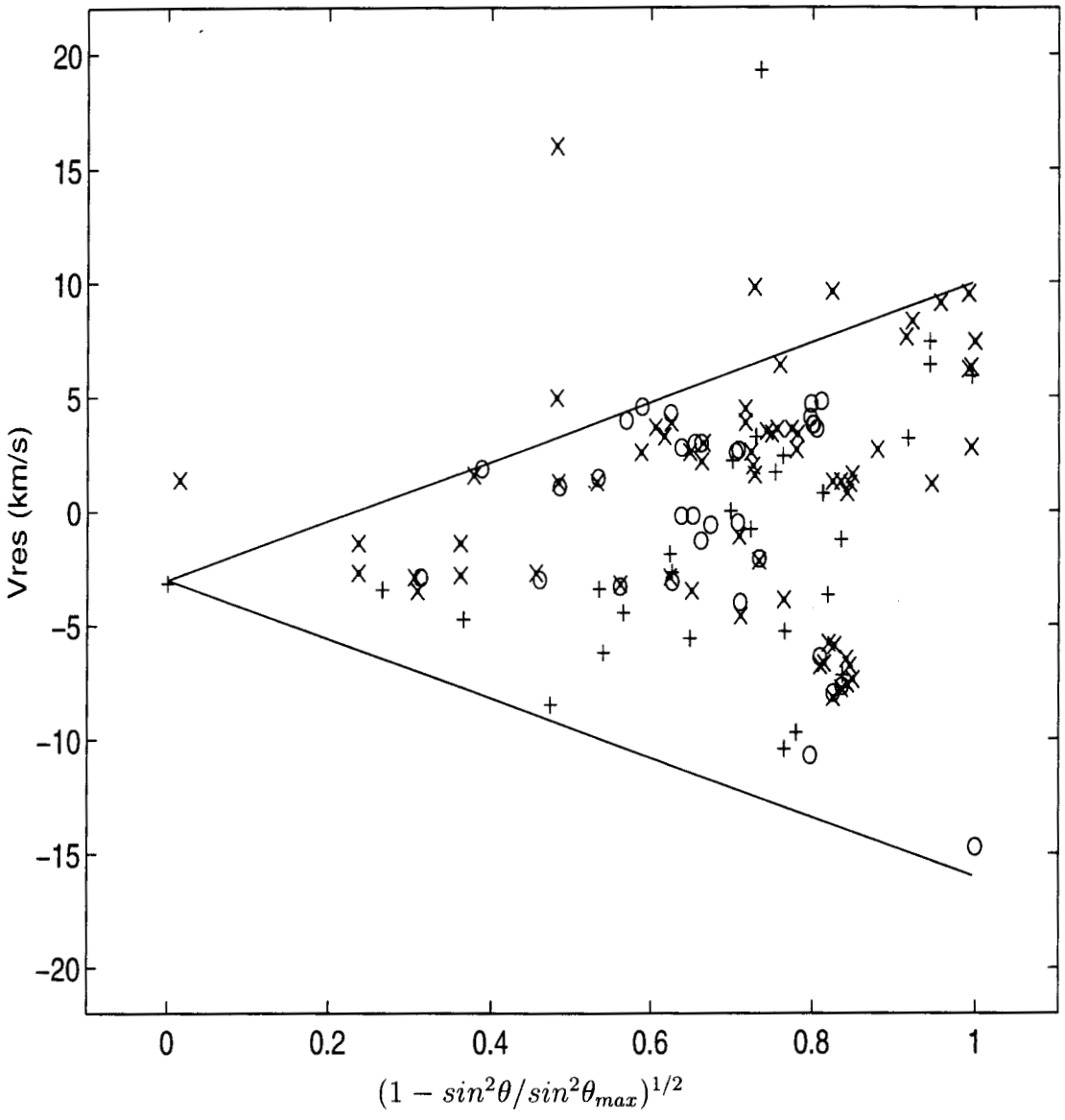

Figure 2.11: **(b)** The residual velocity plotted against $(1 - sin^2\theta/sin^2\theta_{max})^{1/2}$ for ***all*** objects. The plot is the same as Fig 2.11a, except that *the offset* ***for*** *the envelope* ***is - 3*** $km\ s^{-1}$.

plot of the same quantities as in Fig 2.10, but with the Cometary Globules as well as the SDCs included. We have limited the range in galactic latitude to those objects with b < -4" for the same reasons mentioned above. All the Cometary Globules, however, have been included since they form a well defined population with little possibility of contamination. The signature of expansion has clearly been enhanced as a result of the inclusion of the Cometary Globules and SDCs indicating that they belong to the Shell population as well., The envelopes shown are the same as in Fig 2.10 and corresponds to an expansion velocity of 13 km $s^{-1}$with offsets of 0 km s^{-1} (Fig 2.11a) and -3 km s^{-1}(Fig 2.11b). Although it is difficult to decide which envelope "fits" the points better in this case, the statistical tests described in the next section clearly indicate that the envelope shown in Fig 2.11b is to be preferred.

2.8.3 Significance tests

As stated earlier, effects such as sparse sampling towards the edge of the Shell could spuriously boost the signature of expansion in the above exercise. To test the significance of the result we did the following. The order of elements in the v_{res} array (Y-axis) was changed at random. These velocities were then plotted against the unchanged X-axis array, in effect attributing to each ordinate a velocity picked at random from our sample, thus "scrambling" the velocity (v_{res}) axis. This would preserve the effects of any uneven sampling in the abscissa, while randomising the ordinates. In this scrambled plot, the fraction of points satisfying

$$\|v_{res} + v_{offset}\| < v_{exp}(1 - \sin^2\theta/\sin^2\theta_{max})^{1/2}$$

is determined, where v_{offset} is the offset added to each velocity to account for any motion of the Shell as a whole. The mean fraction is found from a large number of such trials. We then look at the deviation of our sample fraction from this random mean. The center of expansion was kept as the morphological center of the Cometary Globules, and the Shell radius chosen was 12.5" as estimated from Fig 2.6. The values of v_{exp}, and v_{offset} were chosen in the following fashion. We determined the minimum value of v_{exp} for which most ($\sim$ 95%) of the points in Fig 2.11 would be inside the "expansion envelope" schematically shown in Fig 2.9b. This was done for a range of values for v_{offset}. The significance test was then done for each v_{offset} and the corresponding v_{exp}. Since the expected Galactic rotation velocity component in this direction (l$\sim$ 263°) is positive, objects with a large positive radial velocity are likely to be beyond the Shell. To reduce this

contamination, we've imposed a cut-off for velocities beyond +15 km s^{-1}. We've chosen this value since the largest negative velocity measured (which cannot be attributed to Galactic rotation and is therefore likely to be a genuine result of expansion) is -15 km s^{-1}.

These tests revealed that the expansion is significant, with the maximum deviation of the sample fraction being 3.3σ from the random mean, for v_{offset} of 3 km s^{-1} and v_{exp} of 13 km s^{-1} which are the values for which the envelope in Figs 2.10b and 2.11b is drawn (for comparison Figs 2.10a and 2.11a show the envelope with no *offset*). Fig 2.12a shows a histogram of this set of trials (for 400,000 trials), with the ordinates showing the fraction of points inside the envelope. The arrow marks fraction of points falling within the envelope in our observed sample. For comparison, in Fig 2.12b and 2.12c, we show the histograms for trials with offsets of 1, 0, -2 and -4 kms^{-1}, all with 13 kms^{-1} expansion velocity. These plots show that the deviation of the fraction of points within the envelope for the observed sample (shown by the arrow in each plot) peaks at the offset ~ -3 km $s^{-1}$and falls off on either side of this value. The picture that emerges is consistent with the SDCs, as well as the molecular material associated with the IPSC sources, forming an expanding shell of $\sim$ 12.5" radius, centered at the morphological center of the Cometary Globules. The entire Shell appears to have a radial velocity of $\sim$ 3 km s^{-1}.

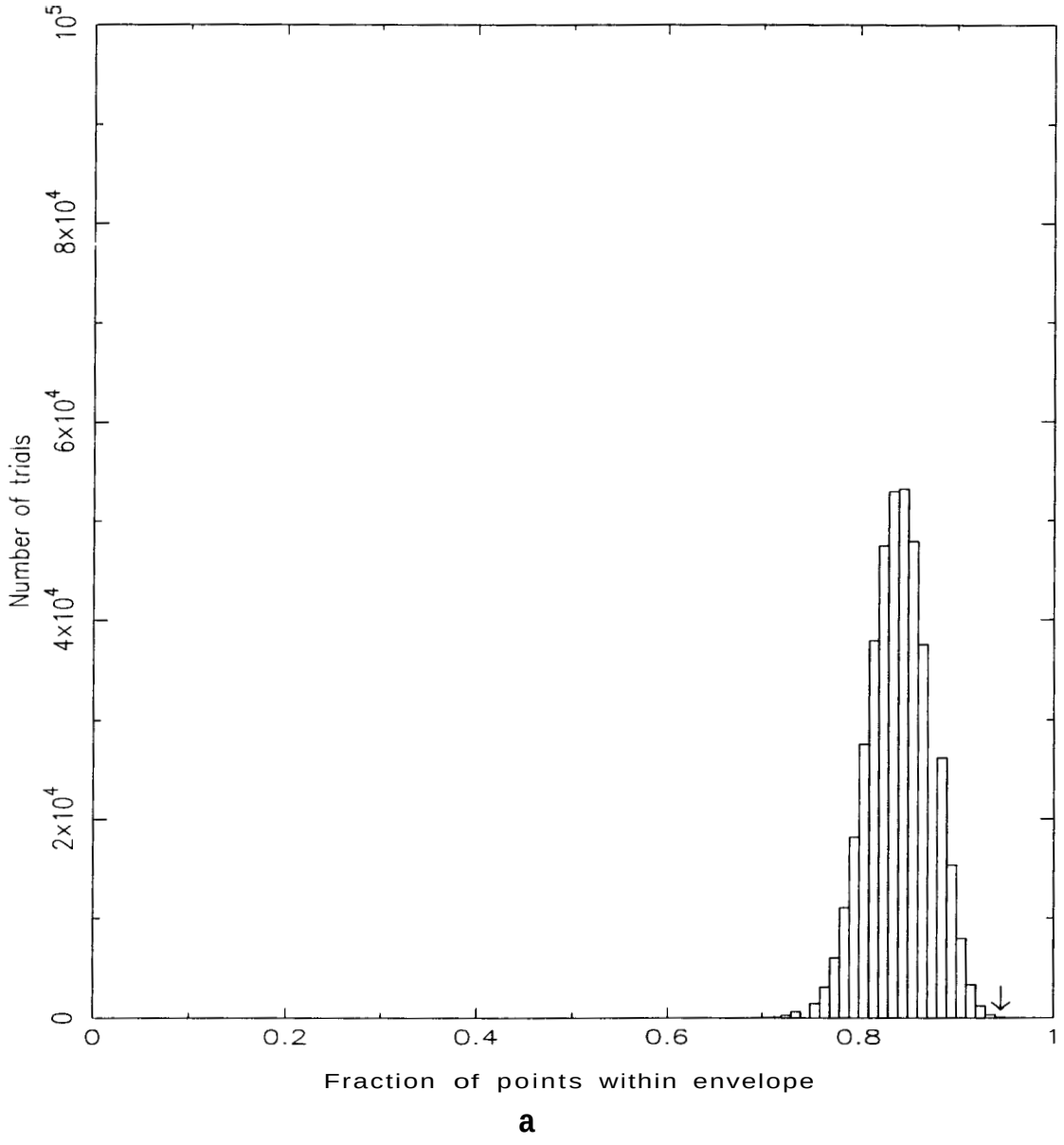

Figure 2.12: Result of significance tests done for an expansion velocity of 13 km s^{-1} and offset of -3 km s^{-1}. In these tests, the velocity axis in the V_{LSR} vs $(1-\sin^2\theta/\sin^2\theta_{max})^{1/2}$ diagram was "scrambled" and the number of points within the "expansion envelope" computed for each trial. The peak of the histogram shows the most likely fraction of points within the "expansion envelope" for a *random sample*. The arrow points to the fraction of points within the "expansion envelope" for the *observed sample*. This point lies **3.3** σ away from the peak for the random samples.

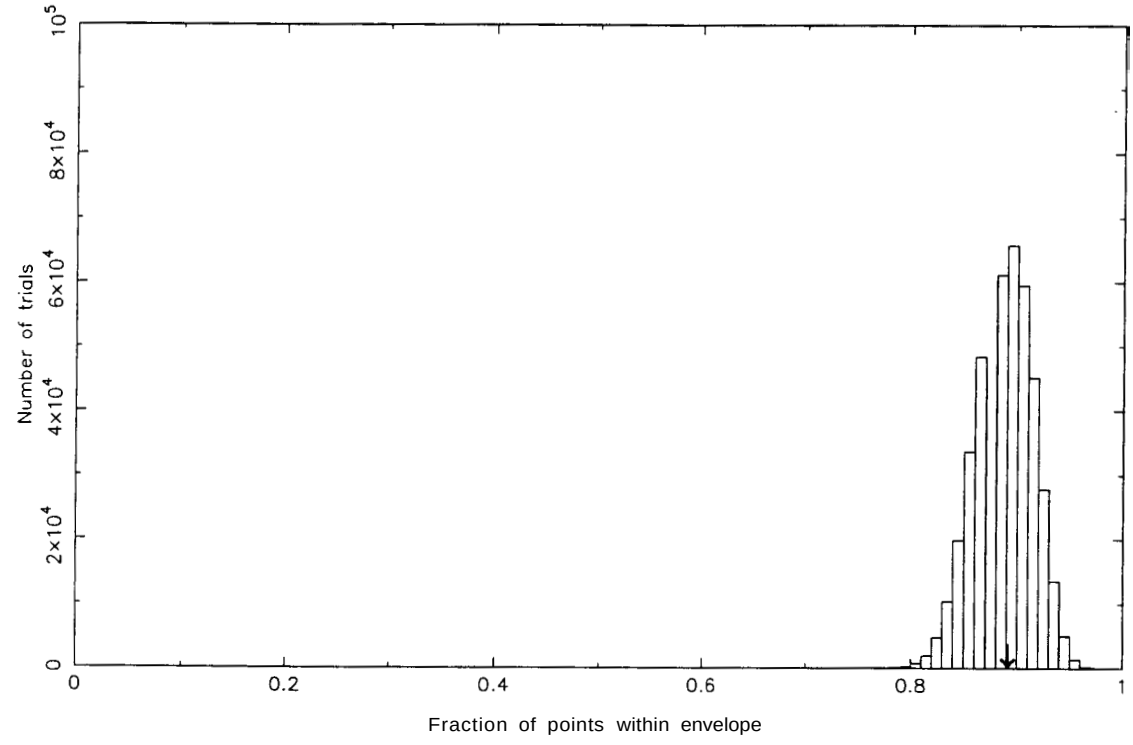

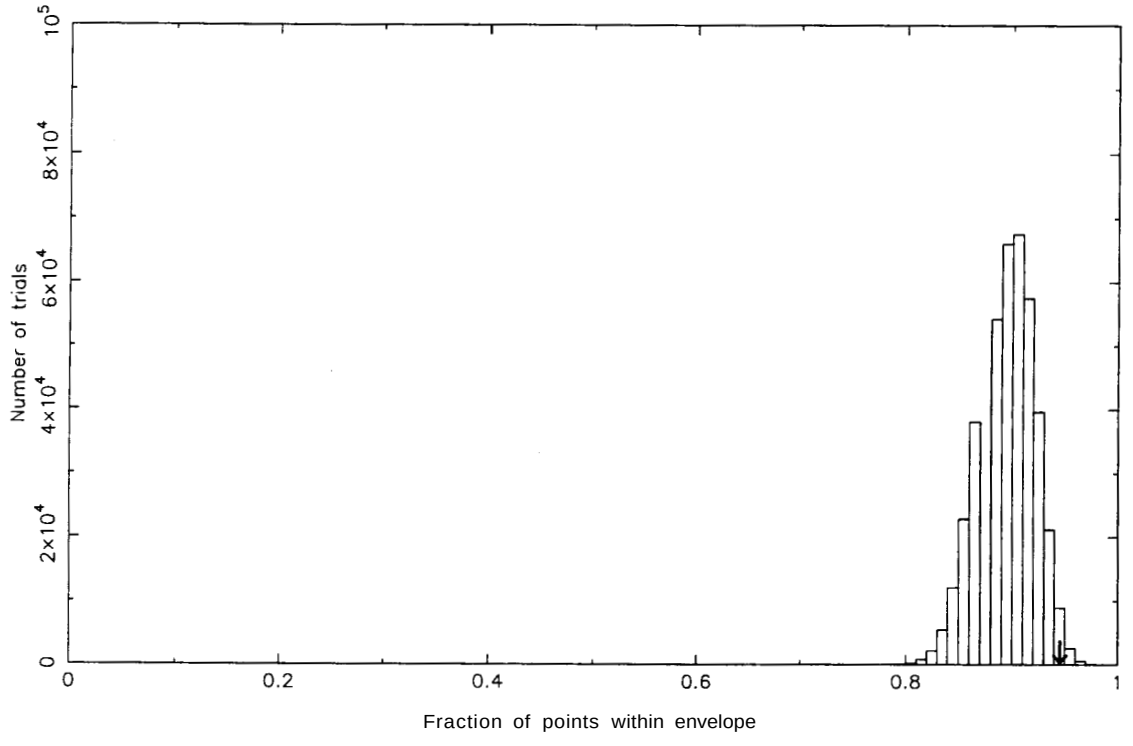

b

Figure 2.12: Result of significance tests done for an expansion velocity of 13 km s^{-1} and offset of 1 (top) and 0 (bottom) km s^{-1}. The arrow points to the fraction of points within the "expansion envelope" for the observed sample. The deviation from the peak for offsets of 1 and 0 km s^{-1} are 0.120 and 1.98σ respectively.

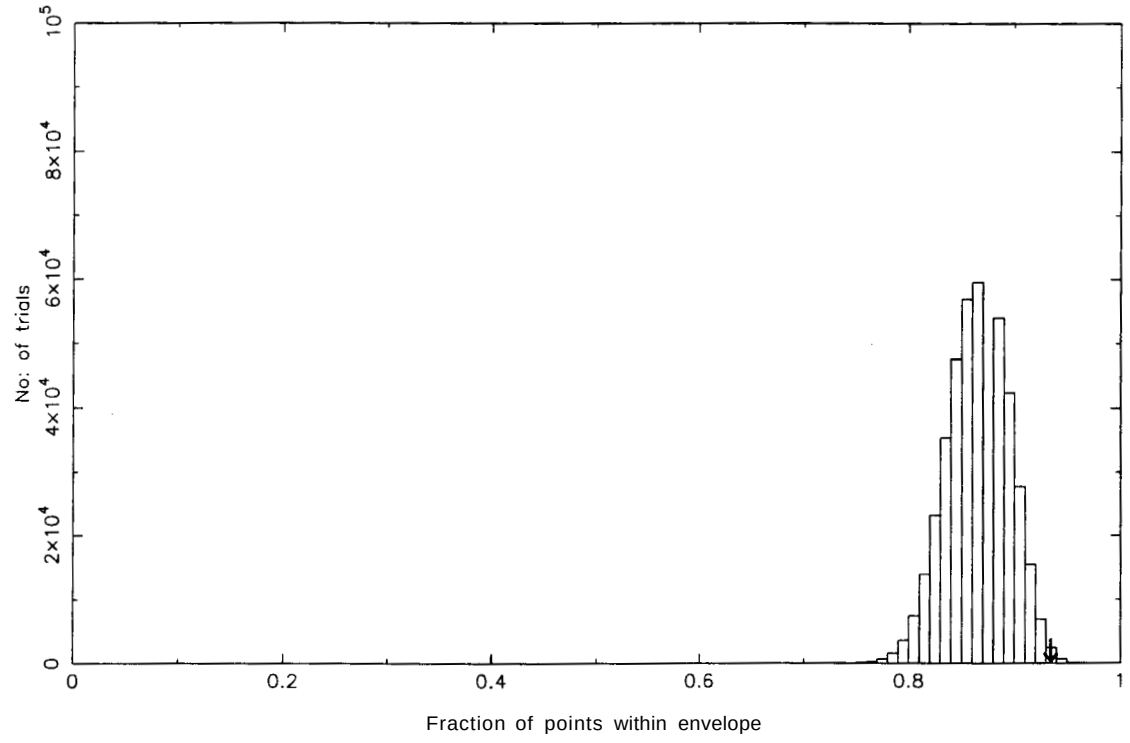

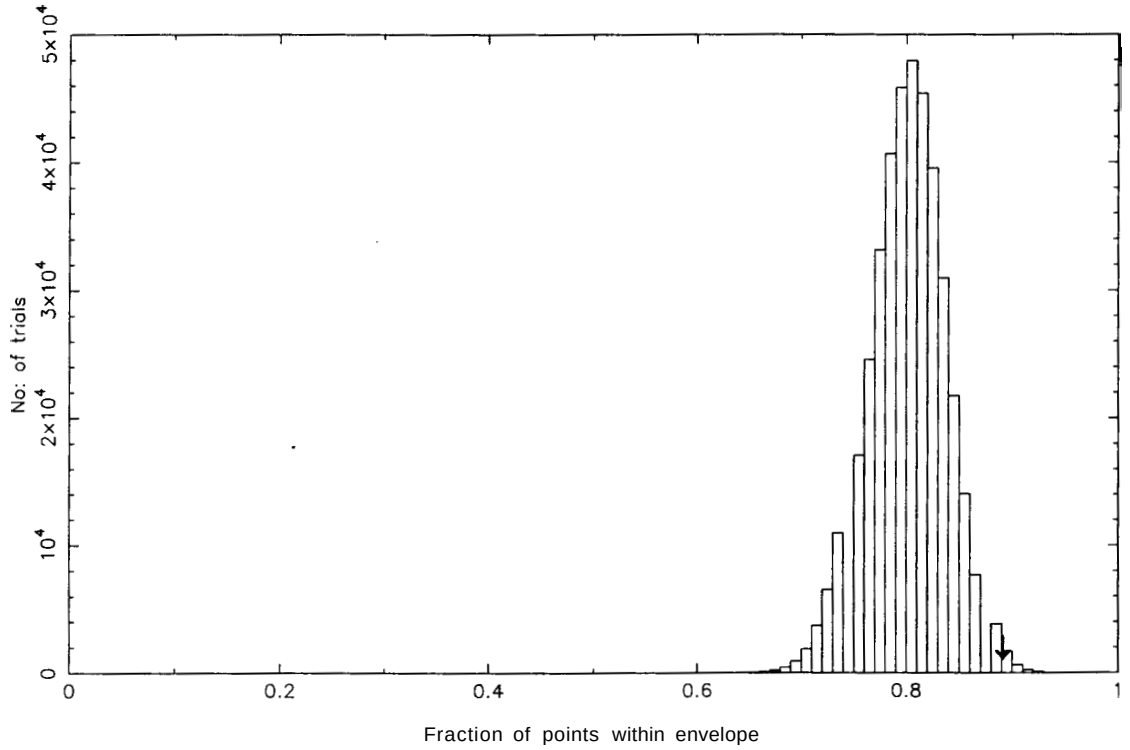

c

Figure 2.12: Result of significance tests done for an expansion velocity of **13** km s^{-1} and offset of **−2** (top) and −4 (bottom) km s^{-1}. The arrow points to the fraction of points within the "expansion envelope" for the observed sample. The deviation from the peak for offets of −2 and −4 are 2.400 and 2.490 respectively.

2.9 Conclusions

Our study in the region of the IRAS Vela Shell reveals the following.

1. There is a significant amount of molecular material associated with the IRAS Point Sources defining the Shell-like feature.

2. The Southern Dark Clouds seen in this region are associated with this Shell and are clearly participating in the expansion.

3. The molecular gas associated with the Young Stellar Objects, the Dark Clouds and the Cometary Globules is expanding with a velocity of $\sim$ 13 km s^{-1}. The center of expansion is close to the "morphological centre" of the system of Cometary Globules, **i.e.**, the location to which the tails of the Cometary Globules extrapolate to. There is evidence for such an expansion in earlier studies of ionised gas in the region, as well as of the system of Cometary Globules.

2.10 Discussion

2.10.1 Molecular gas associated with the IRAS Vela Shell

In this section, we attempt to estimate the mass of molecular material in the expanding Shell of dust and gas described above. Previous attempts to do so have been based on the infrared flux from the dust presumably associated with the Shell. As briefly described in the Introduction, Sahu (1992) estimated the amount of dust and used a dust-to-gas ratio to arrive at a mass estimate for the Shell $\sim 10^6$ $M_\odot$.

Mass estimate of the molecular Shell

We attempt to estimate the mass using two methods:

1. By assuming a typical mass for the objects which constitute the expanding Shell.

2. From an estimate for the star formation efficiency and the number of YSOs in the Shell.

1. Typical mass of the cloudlets

The distribution of molecular gas in the shell is non-uniform and fragmented as can be seen from Fig 2.5. The crosses in the figure indicate non-detections and the circles indicate detection of molecular material from our observations towards the IRPSC sources. The crosses and circles are interspersed with one another, indicating the clumpiness in the distribution of molecular gas.

Detailed studies have been done on the Cometary Globules seen coincident with the Shell and sharing its kinematics. The masses of several of them have been estimated (see Sridharan, 1992, and references therein). They are generally $< 100 M_{\odot}$, with the typical mass being of the order of 20 to $40 M_{\odot}$. Low mass star formation has been confirmed in several of these globules (Bhatt 1993) and these have been identified with IRPSC sources. We shall first estimate the mass of the Shell assuming the clumps of material seen as IRPSC sources in the Shell to be similar to these Cometary Globules. In order to do so, we use the selection criteria defined in section 2.3 to identify the YSO candidates from the IRPSC sources seen in the region. We then identify all those YSO candidates within 12.5" of the assumed center of the Shell. In doing so, we restrict ourselves only to the lower half of the Shell $(b < -4^{\circ})$, which is hopefully free from the contamination from the Galactic plane objects unconnected with the Shell. Further, we take only half this number since our success rate in finding molecular material towards IRPSC sources which satisfy the YSO criteria was of the order of 50%. If we assume an upper limit of 100 $M_{\odot}$ for each of these objects, **the mass of the Shell in molecular gas is $\sim 10^5$ $M_{\odot}$ for the entire Shell** (doubling the mass found in the lower half).

2. Mass estimate from star formation efficiency

A mass estimate for the Shell can also be made from the star formation efficiency. Low mass star formation is known to occur in the Gum region and is plainly evident from the number of YSO candidates seen in the Shell ($\sim$ 1000). The overall star formation efficiency in the local Giant Molecular Cloud complexes like Orion, Ophiuchus and Taurus-Auriga is $\sim$ 1% (Evans and Lada 1990). The efficiency in the Shell is likely to be larger (as high as a 10% or more, if one goes by the efficiency seen in Cometary Globules; Bhatt, 1993). However, we adopt this value of 1% to arrive at an upper limit to the Shell mass. We assume the typical mass of a star formed in this region to be 1 $M_{\odot}$. For the young star seen inside the globule Cometary Globule22, the mass estimate is in the range of 0.6

to 2 $M_\odot$ (Sahu 1992). Thus the adopted typical value of 1 $M_\odot$ is a reasonable estimate. We identify YSOs using the same criterion as in the method described above and estimate the total mass of stars in the entire Shell to be $\sim$ 100 $M_\odot$. The mass **of** the Shell is thus $\sim 10^5 M_\odot$, consistent with the estimate made in the preceding section.

These estimates refer primarily to the molecular gas in the Shell. There is also evidence for ionised gas in the region, seen as an excess of Hα emission coincident with the Shell inside the Gum Nebula, and also from emission lines from ionised species like NII, SII etc. No clear evidence exists for neutral gas towards the Shell as a whole. Lyman α absorption measurement towards γ^2 Velorum by the Copernicus satellite yielded a column density of $\sim 10^{19}$ cm^{-2} in this direction. However, as we point out later the recent Hipparcos distance measurement towards this star places it in the foreground of the Shell. In a recent study by Dubner et *al.*(1992) a thick HI *shell* has been identified from 21 cm emission measurements towards the Gum Nebula. This HI shell is however not coincident with the molecular Shell, although there is some overlap in projection. An HI *disk* is also seen in the velocity range of 0 to 10 kms^{-1}, which is the radial component of Galactic rotation expected at a distance of $\sim$ 400 pc, i.e the assumed distance to the Gum Nebula. This large disk is of similar size and seems coincident with the Nebula. Neither of these features can be confidently identified with our molecular Shell. Thus one can make no statement at present about the neutral gas associated with the molecular Shell. We shall return to this question a little later. Given this situation, the mass of gas in ionised and neutral form is difficult to estimate. However, our estimates of the gas mass tend to overestimate the mass in molecular form and therefore the total mass of the Shell is not likely to exceed this estimated mass of $10^5 M_\odot$ significantly.

2.10.2 On **Hipparcos Distances**

Before we discuss the possible nature and origin of the molecular Shell, we summarize the new distance estimates to some of the stars in the region which play an important role in all interpretations of the various features seen in the region. The Hipparcos mission was launched in 1989 to do precision astrometry from space. The measured parallax has improved the accuracy in position of the target stars by as as much as a factor of hundred, to the order of 1 milli-arcsecond. de Zeeuw *et al.*(1997) have used the Hipparcos mission to identify members of nearby OB associations through proper motion, parallax and position studies. The mem-

bership of these associations are now established down to late F spectral class. Preliminary results from this study has established several important facts about the Vela OB2 association.

1. This group of stars is now established as a bona-fide association with a membership of 116 stars, including γ^2Velorum, from proper motion studies.

2. Of the 116 members only one, γ^2 Velorum, is an O star the rest being B or later spectral type.

3. Only 4 out of the 10 stars originally thought to constitute the association (Brandt *et al.*1971) are confirmed as members.

4. Hipparcos parallax measurements have also established the distance to ζ Puppis and y^2 Velorum. The distance to ζ Puppis is 429^{+120}_{-77} pc and that to γ^2 Velorum is 258^{+41}_{-31} pc (Van der Hucht et *al.*197l). The latter casts doubt on whether γ^2 Velorum is a member of Vela OB2, despite the matching proper motion.

Fig 2.13 from de Zeeuw *et al.*(1997) shows the identified members of Vela OB2, along with their proper motions. The IRAS Vela Shell as seen in the IRAS Sky Survey Atlas is also shown. The mean distance to Vela OB2 is 415±10 pc. A separate study (Schaerer, Schmutz and Grenon 1997), also based on Hipparcos results, favours an age of $\sim 10^7$ years for the bulk of the stars in Vela OB2. **These results confirm that Vela OB2 is a genuine fairly evolved association at ~415 pc.**

We shall use these new results in the following discussion of the nature of the Gum Nebula and the molecular Shell.

2.10.3 On the nature of the expanding Shell of gas and dust

The interstellar medium in the Gum-Vela region shows several structures when viewed in different wavelengths. Disentangling these from each other and establishing their true nature and origin have proved difficult. In this section we attempt to put the molecular Shell in perspective against the present understanding of the region, and comment on its possible origin.

To recall, our study has established the following:

- **There is a Shell of molecular gas associated with the IRAS Vela Shell in the Gum-Vela region.**

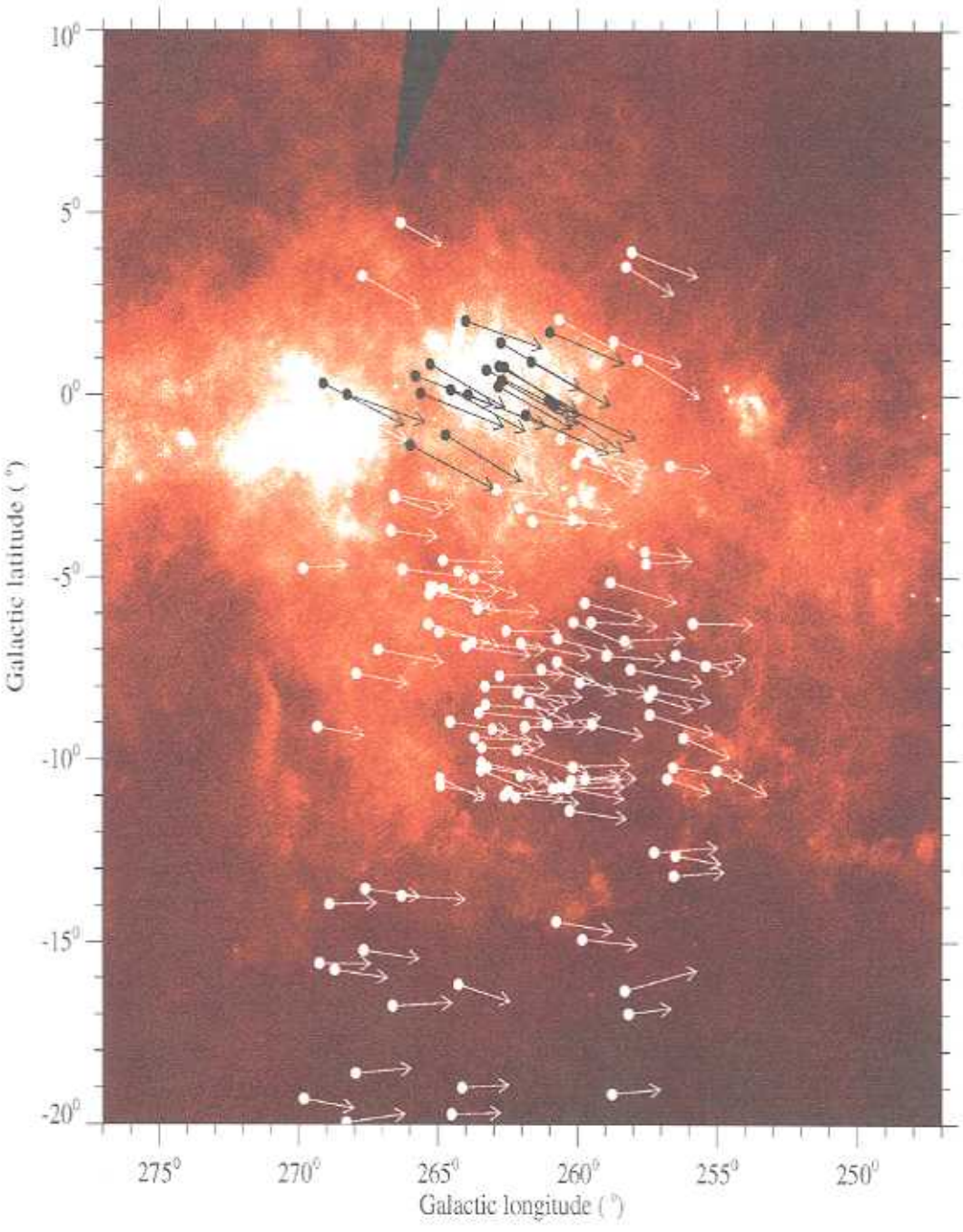

Figure 2.13: Proper motions in the Vela OB2 association superimposed on a colour representation of the IRAS 100μm skyflux. The white dots show the Vela OB2 members and the black dots show the members of Trumpler 10, another group in the Vela OB2 field located at a distance of $\sim$ 360 pc. The core of the Vela OB2 association is sorrounded by the IRAS Vela Shell. From de Zeeuw *et al.*(1997).

- **We estimate the mass of gas in the Shell to be $\sim 10^5$ $M_\odot$.**

- **The Shell is expanding with a velocity of $\sim$ 13 km s^{-1}.**

The Shell envelopes the Vela OB2 association. Fig 2.14 adapted from Sahu (1992) shows the various objects in the region, including Vela OB2, and the bright stars ζ Puppis and γ^2 Velorum. The envelope of the molecular Shell is also shown. Recent Hipparcos results show that Vela OB2 (shown as open circles) is a fairly evolved ($\sim 10^7$ years) association at a distance of $\sim$ 415 pc. Based on these facts we conclude that the molecular Shell which appears as expanding clumps of molecular gas *is the remnant of the parent Giant Molecular Cloud which gave rise to the Vela OB2 association.* The Giant Molecular Cloud was presumably broken up and is being swept out by the combined effect of supernova explosions, UV radiation and stellar winds. This scenario had also been advanced by Sahu (1992) for the formation of the IRAS Vela Shell. She estimated that the energy input from Vela OB2, assuming it to be a "standard" association in the absence of detailed knowledge of its membership at the time, was consistent with the energy requirement for the expanding IRAS Vela Shell following the theory of "supershells" formed around OB associations by McCray and Kafatos (1987).

We now describe some observational evidence as well as theoretical arguments to support the hypothesis that the break up of Giant Molecular Clouds in this fashion is a common event.

- Most OB associations in the Solar neighbourhood are associated with Giant Molecular Clouds. In a systematic survey of ^{12}CO emission from the neighbourhood of **34** clusters, Leisawitz, Bash and Thaddeus (1989) established that most of the molecular clouds associated with the clusters show systematic recession velocities of $\sim$ 10 km s^{-1} or so. This can directly be attributed to the result of interaction with the cluster. They also find evidence for the *partial dissolution of the clouds.* The clouds exhibit bright rims, possibly as a result of the interaction with the bright stars in the cluster. There is also evidence for streaming flows of ionised gas, pointing to ablation of the clouds exposed to UV radiation, stellar winds, and evaporation inside hot "bubbles" created by stars. The molecular gas is seen to be in "clumps". All these point to the fragmentation of the clouds. Star formation is also observed to take place in all these regions, with the ratio of stellar mass to total mass in regions around young clusters to be $\sim$ 1 to 2 %.

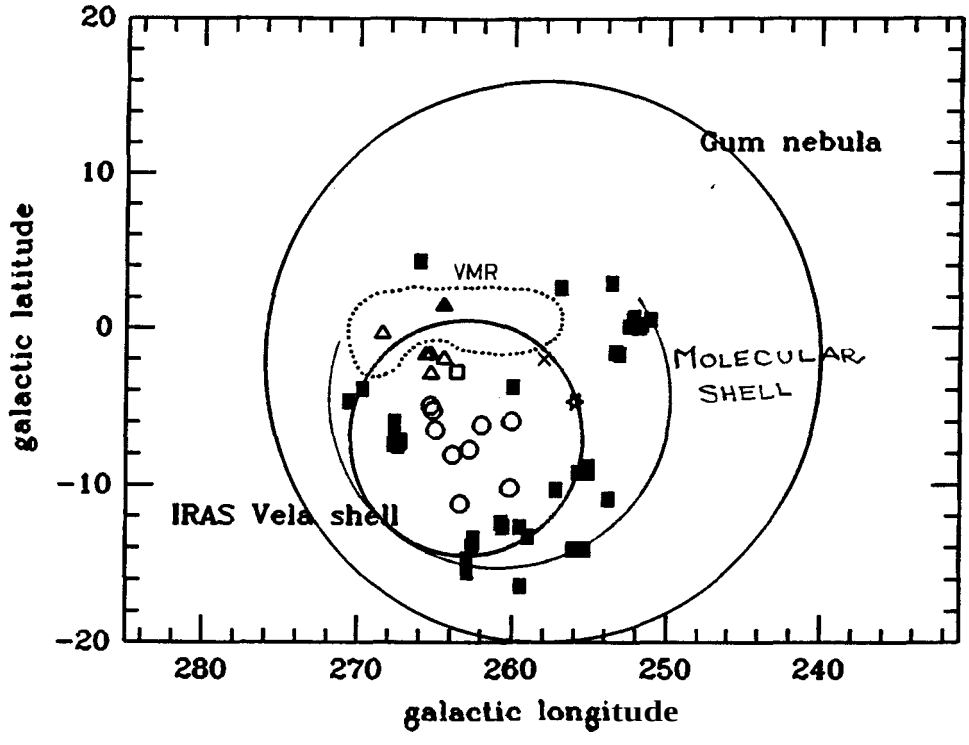

Figure 2.14: Schematic of locations of IRAS Vela Shell, Gum Nebula, Vela OB2, Vela R2, Cometary Globules and Vela Molecular Ridge as they appear in the sky (reproduced from Sahu 1992). The Vela OB2 stars are shown by open circles, the average location of the Vela R2 stars is shown by a filled triangle, ζ Puppis is shown by a "star", the Vela pulsar by an open square and the Vela OB1 stars by open triangles. The filled squares indicate the location of the CGs and some dark clouds in the region. The dotted region is the Vela Molecular Ridge and the center of the Gum Nebula on Hα photographs is shown by a cross. We indicate also the outer envelope of the molecular Shell by a circle.

- Bally and Scoville (1980) found evidence for an expanding network of clouds around an old HII region, W80. The expanding shell has a velocity of around 5 km s^{-1}. Again, there is evidence for star formation and fragmentation. They attribute this shell as resulting from the destruction of a part of a larger molecular cloud due to the interaction with the HII region of a bright star formed inside the cloud. Bally et *al.*(1990) have reviewed these and other observational evidence for the interaction of OB associations with parent clouds.

- An archetypal example of a Giant Molecular Cloud associated with star formation is of course the Orion complex. We present some of the evidence for the break up of Giant Molecular Cloud from observations in the Orion region and estimates for the energy input to the clouds from the neighbouring stars. The Orion A and B clouds, along with 14 smaller clouds in the region, show evidence on the large scale for compression, acceleration, ablation and dispersion of molecular gas over a period of 10^7 years. We summarize some of these signs of disruption.

  - The molecular gas is seen in filaments and partial shells.

  - Large scale velocity gradients, cloud shapes and orientations point towards the center of the Orion OB1 association.

  - The sphere of influence of the Orion OB1 association extends to a region 100 pc x 300 pc in size, enveloped by a large expanding HI shell

  - At least 16 clouds in the region exhibit cometary morphology. Some of these are fairly large clouds. All these clouds "point" towards the center of Orion OB1. Two of these globules are as far away as 15° from the center of Orion OB1, and are $\sim$ 300 pc from the galactic plane. They could have been ejected from the center or condensed from the HI shell.

  - Active star formation is seen in the dense gas near the OB association. Dense concentrations of embedded objects are seen with 50 to 1000 members each.

Further details of these remarkable phenomena can be found in the review by Bally et *al.*(1990). The major interaction between star clusters and parent Giant Molecular Clouds take the form of shock waves associated with outflows

from embedded objects, stellar winds, supernovae and UV radiation. The energy input from outflows is relevant only over small scales of less than a parsec.

During the past 10^7 years, several dozen O stars must have exploded as supernovae in Orion (Blaauw 1964, 1984), releasing about 10^{51} ergs every 5×10^5 years or so. Moreover, these stars have already injected a comparable amount of energy into the ISM in the form of stellar winds during their lifetime. The energy input from the Orion OB association is therefore at least of the order of 2×10^{51} ergs per 5×10^5 years, or a mechanical luminosity of $\sim 3\times10^4$ $L_\odot$. Assuming an efficiency of $\sim .003$ for conversion of this energy into motion (Bally *et al.,* 1990) and if the clouds are assumed to subtend 10% of the sky as seen by the OB association, the kinetic energy injection rate into the clouds from supernovae is of the order of 10 $L_\odot$. These together sweep out "supershells" of HI as discussed later in this section. The interiors of these shells are periodically energised by supernovae and are believed to be at temperatures of $\sim 10^6$ K. The clouds enveloped by the shells undergo evaporation by heat conduction at the surface.

The luminosity of Orion in Lyman-a photons is $\sim 2\times 10^{49}$ photons s^{-1}. If the clouds subtend 10% of the sky as seen from the stars, this translates to > 10 $L_\odot$ kinetic energy injection rate from UV radiation (assuming an efficiency of .001 for converting the ionizing radiation into motion). Hence the UV radiation energy input is comparable to the supernovae and stellar wind input. The UV radiation heats up and ionises the sorrounding gas. "Champagne flows" of ionised gas are observed in star forming regions (Bodenheimer, Tenorio-Tagle and York 1979). These streaming flow of ionised gas is seen at velocities close to the sound speed in ionised gas (~ 10 km s^{-1}). The resulting "rocket effect" (Oort and Spitzer 1955, see chapter 1) can accelerate the clouds to a velocity $V = C_{HII}M_{HII}/M_{neutral}$ where C_{HII} is the sound speed in ionised gas. Clouds can be accelerated to near the sound speed of ionised gas (Bally and Scoville 1980).

The effects of stellar winds, supernovae and UV radiation is seen in almost all **Giant Molecular Cloud-OB associations** near the sun. Per OB2 and Sco-Cen are two nearby OB associations which have large HI shells associated with them. All clouds within 700 pc of the sun with mass $> 10^4$ $M_\odot$ have OB associations and neutral hydrogen shells.

From the above discussion it is clear that the molecular Shell in Vela exhibits many of the signatures of being the remnant of a broken up Giant Molecular Cloud. *Cometary globules with bright rims which show signs of the "rocket effect", an expanding shell of molecular gas, the fragmented appearance with the*

gas distributed in clumps, etc are some of the evidence. There is also evidence for expanding ionised gas which is expected as a result of the ablation of the cloud, but as mentioned earlier the spectroscopic study of ionised gas has so far been limited to only a few directions towards the Shell. Here we recall that our analysis also reveals an overall drift velocity (~ 3 km s^{-1}) of the Shell as a whole. This motion could be attributed to the velocity of the original Giant Molecular Cloud itself. If this is true, it has an interesting implication for the member stars of the Vela OB2 association, which should also share this motion. Admittedly, a component of this small magnitude is difficult to detect among the stars of what is already a loosely associated group with a large dispersion of distances and motion. We estimated the mass of the Shell to be 10^5 $M_\odot$, from both the measured masses of dark clouds (Cometary Globules) seen in the region as well as from star formation efficiency considerations. The mass estimated by Sahu from dust-to-gas ratio calculations is of the order of $10^6 M_\odot$. This appears to us to be an overestimate. Our estimate is also consistent with the accepted mass range of Giant Molecular Clouds and therefore with the assumption that the Shell is the remnant of a Giant Molecular Cloud.

An earlier study of the Cometary Globules seen in the region by Sridharan (1992) had led him to conclude that these globules of molecular gas, which show a peculiar head-tail morphology and bright ionized rims, could be the remnants of a Giant Molecular Cloud which gave birth to the Vela OB2 association. We now confirm the presence of exactly such a remnant in the form of a large expanding ring of molecular gas.

In the subsequent discussion, we shall assume that the distance to the Shell is $\sim$415 pc, the mean distance to the Vela OB2 association. At this distance the maximum observed angular radius of the Shell of $\sim$ 12.5" translates to a linear radius of 80 to 90 pc. "Super shells" are large ring-like structures seen in our Galaxy and external galaxies (Heiles 1979, 1984). These have been conjectured to be formed from the interstellar medium swept up by supernovae and stellar winds from stars in OB associations (McCray and Kafatos, 1987). The energy input to the interstellar medium from an OB association can be estimated if one knows the mass function of the member stars and age of the association. OB associations are invariably formed in and found in the vicinity of Giant Molecular Clouds. The interaction of the stellar winds and supernovae from these clusters of stars therefore is initially with the parent molecular cloud itself. The formation of a super shell from swept-up interstellar medium must therefore be preceded by

the break-up and expansion of the Giant Molecular Cloud. The disrupted parent cloud is swept aside and the expanding Shell sweeps up more interstellar medium. The Vela Shell is a prime candidate for such a scenario. Later in this section we discuss the present age, mass swept up so far, and the possible future evolution of such a shell. We now go on to discuss the system of Cometary Globules seen in the region.

Are the Cometary Globules part of the Shell?

As was stated in the previous discussion, the system of Cometary Globules are seen distributed along the Shell. They are molecular clouds with bright ionized rims (we discuss these rims and in particular one of the largest Cometary Globules, CG22 in Chapter 4) and faintly luminous tails. Their masses are of the order of 20 $M_{\odot}$, and the sizes of the Cometary Globule heads are $\sim$ 0.1 pc or so, although the tails can be extended. The tails are seen to point away from a common center. The kinematics of the molecular gas in the Cometary Globules was studied by Sridharan (1992). His analysis reveals that this system of clouds are expanding about their morphological center (indicated in Fig 2.8) with a velocity of $\sim$ 12 km s^{-1}. The implied expansion age is of the order of 6 x 10^6 years. The Cometary Globules also show a velocity gradient from head to tail. From this the estimated age for tail formation is $\sim$ 3x 10^6 years. Enhanced star formation is known to occur in the Cometary Globule heads. From his study, Sridharan concluded that the Cometary Globule system was associated with ζ Puppis and possibly γ^2 Velorum. To summarize some of his findings:

- The morphological center of the Cometary Globules is close to the projected path of ζ Puppis in the past. From the proper motion of ζ Puppis, it was closest to the Cometary Globule center about half a million years ago.

- The present expansion of the Cometary Globules can be accounted for as being caused by stellar winds, radiation pressure and the "rocket effect" due to ζ Puppis alone.

- The bright rims of the Cometary Globules are likely to be caused by radiation from ζ Puppis.

Given the clear association of ζ Puppis and the Cometary Globules, the distance to the Cometary Globules should be $\sim$ 450 pc. Independent distance estimates also place it in this region. Brand et *al.*(1983) have done photometric and

spectroscopic studies of the star CD−44°3318 seen in the head of the Cometary Globule CG1. UBVRI and JHKL photometry confirms that this is a variable star. The flux varies by almost a magnitude while there is little variability in the colour, leading the authors to conclude that the variability is caused by extinction in moving dust clouds in the remnants of the prestellar nebula. From the maximum V magnitude and assuming values for the extinction E(B-V) and the total to selective extinction ($A_v/E(B-V)$), they arrive at an absolute magnitude $M_v = 1.2 \pm 0.6$. The distance estimate from this value is $\sim$ 500 pc, with large uncertainty. The photometric distance estimate to the anonymous GO-5V star seen towards the dark cloud DC 253.6−1.3, associated with the Cometary Globule 30-31 complex is 460±40 pc (Pettersson 1987). The moderate reddening towards this star makes it likely that it is in the foreground of the cloud and the distance is a lower limit to the Cometary Globules. These estimates place the Cometary Globule system in the vicinity of the molecular Shell. Given this and the fact that they share the Shell morphology and expansion, the Cometary Globules can reasonably be assumed to be part of the Shell. The obvious question then is: Why are the Cometary Globules distinct in their head-tail morphology and bright rims as compared to the other clouds (for eg, the SDCs) seen in the Shell ? The answer could lie in what has already been stated. The rims and tail are believed to arise as the result of the interaction with the nearby O star ζ Puppis. It seems likely that only the clouds close to this star are seen as Cometary Globules. In Fig 2.15, we sketch such a possible configuration for which only the clouds near ζ Puppis have tails. Given projection effects, it is difficult to verify this conjecture.

Vela OB2 is a fairly evolved association. The age of the molecular Shell is also likely to be of the same order. ζ Puppis is a young supergiant ($\sim 10^6$ years, Sahu(1992)). Therefore the Cometary Globules, if associated with this star are likely to be a recent phenomenon compared to the entire Shell.

2.10.4 The Gum Nebula

The most striking enigma in this part of the sky is of course the Gum Nebula itself. Discovered in 1952 by Colin Gum, this is one of the largest objects seen in the sky, and yet its nature and origin still remain obscure. There are several candidate theories for the nature of the Gum Nebula (review by Bruhweiler et *al.*1983), and we briefly mention the principal ones.

Gum (1956) proposed that the nebula is a large classical HII region ionized by the brightest stars in the region, the 04f star ζ Puppis and the Wolf Rayet-0 star

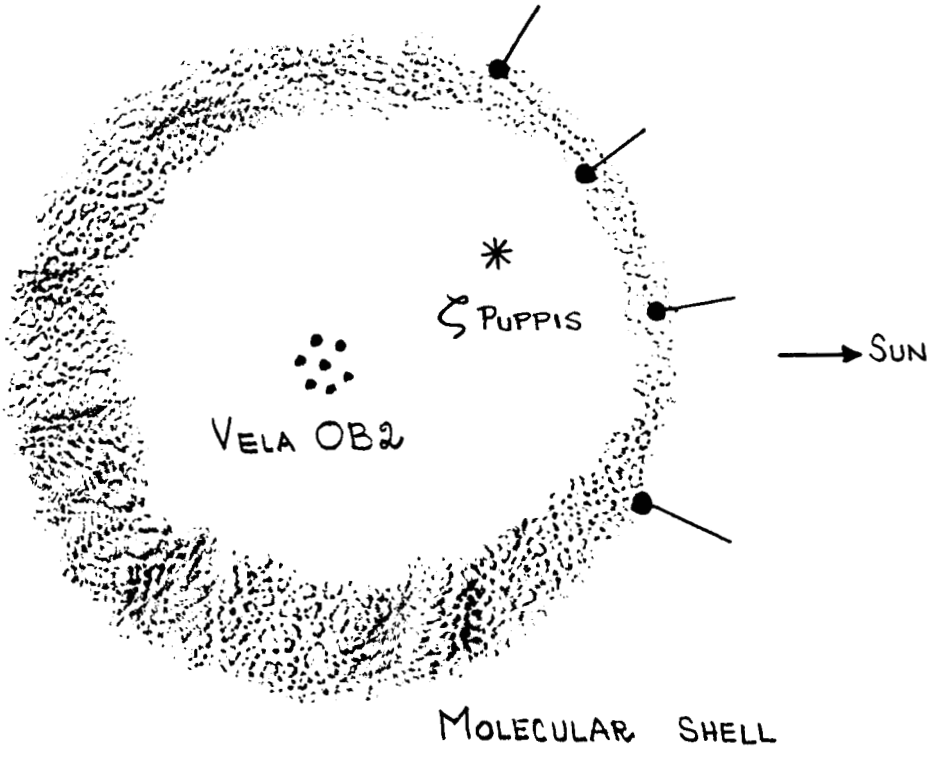

Figure 2.15: Schematic figure showing a possible configuration to explain the presence of Cometary Globules. ζ Puppis is asymmetrically placed inside the molecular Shell and its influence is stronger on the clouds nearer to it, causing them to appear as Cometary Globules with bright rims, while the rest of the Shell is relatively unaffected.

binary γ^2 Velorum. This hypothesis has been supported by Beuerman (1973).

Earlier attempts to estimate the size of the Gum Nebula from its Hα emission (a difficult task because of its extremely faint and diffuse nature) had led to angular sizes as large as 75" x 40" (Brandt et *al.*1971). Since the two bright stars mentioned above are not capable of maintaining an HII region of this size, Brandt et *al.*suggested that the nebula is the "fossil Stromgren sphere" of the Vela supernova event, being currently ionized by ζ Puppis and γ^2 Velorum.

The current and most accurate estimate for the angular size of the nebula is that due to Sivan (1974) through wide field Ha imaging. He estimates the size of the nebula as 36°, smaller than previous estimates. This obviates the necessity to invoke a fossil Stromgren sphere model. Based on spectroscopic study of the ionized gas, Reynolds (1976 a, b) proposed that the nebula is an old SNR heated and ionized by ζ Puppis.

Weaver et *al.*(1977) suggest that the nebula is a shell formed by the interaction of the stellar wind from ζ Puppis and γ^2 Velorum with the ambient interstellar medium. They also predict soft X-rays from the hot ($\sim 10^6$ K) interior.

Wallerstein, Silk and Jenkins (1980) in a detailed study of CaII, NaI and UV lines of sulphur, nitrogen, carbon and silicon towards stars in the Gum Nebula came to the conclusion that the nebula is consistent with a model of an HII region stirred up by multiple stellar winds. Chanot and Sivan (1983) however, support the model of Reynolds (1976b) for an expanding Ha shell ionized by UV flux from ζ Puppis and γ^2 Velorum based on Ha morphology and spectroscopy of ionized gas. The origin of the shell structure however is uncertain. The expansion of the nebula has also been a subject of controversy. Although Reynolds (1976a) claimed an expansion velocity of $\sim$ 20 km s^{-1}, later attempts by Wallerstein, Silk and Jenkins (1980) and Sahu (1992) fail to find conclusive evidence for expansion.

From a detailed study of the region Sahu (1992) came to the conclusion that the nebula is a shell like structure sorrounding the Vela R2 association. This is a young association (Herbst 1975) at an estimated distance of $\sim$ 870 pc. Sahu argues that the Shell has formed through the interaction of the stellar winds and supernovae from Vela R2 with the sorrounding interstellar medium. This argument is based on the location of the nebula with respect to Vela R2 and its estimated kinematics. The Gum Nebula shows no distinct *IR* emission except in the region of the IRAS Vela Shell. The kinematics of the two regions also differ. Based on these facts Sahu concluded that the IRAS Vela Shell and Gum Nebula are two separate entities, apparently associated only because of projection. She placed

the IRAS Vela Shell at $\sim$ 450 pc, the pre-Hipparcos distance estimate for the Vela OB2 association. The Gum Nebula was placed at $\sim$ 800 pc which is the accepted distance to the Vela R2. The primary reason for her assuming this large distance to the Gum Nebula was tied up with the assumed distance to ζ Puppis. This 04f supergiant is accepted to be the primary source of ionisation in the Gum Nebula (Reynolds 1976a, Chanot and Sivan 1983). Sahu questioned the association of this star with Vela OB2 since their ages are disparate. Based on the proper motion study of its members, she concluded that Vela OB2 appears to be an old association ($\sim 2 \times 10^7$ years). ζ Puppis is a young star ($\sim 10^6$ years) proposed to be a runaway star to explain its large space velocity of $\sim$ 70 km s^{-1}(Upton 1971). Since runaway stars are believed to result from a supernova explosion in a binary system (Blaauw 1961), ζ Puppis must have had a massive companion star which exploded as a supernova. This implies that an even more massive star was born in Vela OB2 at roughly the same time as ζ Puppis, aggravating the age discrepancy problem. Tracing back the proper motion of ζ Puppis, its past path runs close to both Vela OB2 and Vela R2 in projection. The distance to ζ Puppis was ill-determined till the recent Hipparcos measurements because of its controversial spectral classification and ranged from $\sim$ 450 (Brandt et *al.*1971, Garmany and Stencel 1992) to 800 pc (Allen 1973). Given this range of possible distance, and the discrepancy in the ages of Vela OB2 and the past companion of ζ Puppis, Sahu concluded that ζ Puppis originated in Vela R2, a younger cluster in which star formation has been going on for a few million years (Herbst, 1975). This would mean that ζ Puppis is $\sim$ 800 pc away. Thus in Sahu's model, the Nebula is completely separate from the IRAS Vela Shell. Fig 2.16 shows a schematic sketch from Sahu (1992) showing the locations of the various objects as in the scenario described above.

The Hipparcos distance to ζ Puppis clearly rules out the above scenario. Almost all models agree that this star is one of the major sources of UV flux to account for the ionisation seen in the Gum Nebula and therefore the nebula has to be in the vicinity of the star i.e, at $\sim$ 450 pc. Our distance estimate to the Shell therefore places it inside or overlapping with the Gum Nebula. The interpretation of the nebula remains a difficult task. Recent HI emission measurements towards the nebula by Reynoso and Dubner (1997) reveal an HI disk possibly associated with the nebula. This has led to the conjecture that the nebula is a super shell formed by the Vela OB2 association. Most of the other models refer to the influence of supernovae and stellar winds on the nebula, albeit

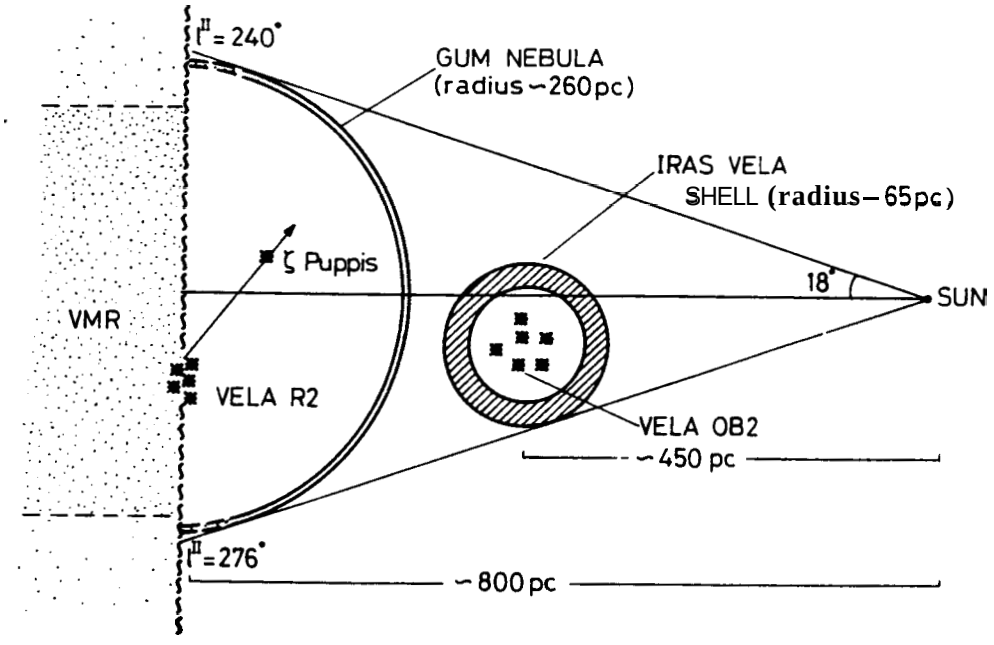

Figure 2.16: The main conclusions from the study by Sahu are schematically shown in this diagram from Sahu (1992). The various objects seen in the Puppis Vela region are shown in the form of a projection onto the Galactic plane. ζ Puppis and its past projected path, Vela OB2 stars and Vela R2 stars are also indicated, along with distances to the IRAS Vela Shell and the Gum Nebula as estimated by Sahu.

without specifically referring to it as a swept up shell. We have argued that the molecular Shell, expanding with a velocity of $\sim$ 13 km s^{-1} is the remnant of the parent Giant Molecular Cloud of Vela OB2. This scenario is difficult to reconcile with an already existing shell, which is nearly twice the size. Hence we question the interpretation of the Gum Nebula as a swept up super shell formed by Vela OB2. The electron density estimate inside the nebula range from .1 to 100 cm^{-3} (Reynolds (1976a), Wallerstein, Silk and Jenkins 1980) and the temperature estimates are all consistent with the average temperature being $< 10^4$ K (Chanot and Sivan (1983), Reynolds (1976a), Wallerstein, Silk and Jenkins (1980)). These values do not appear to indicate that the entire nebula is the interior of a stellar wind bubble or a supernova bubble. There is enhanced $H\alpha$ emission from the region of the IRAS Shell. The temperature estimates from line widths of the NII and Ha line at the periphery of the Shell are again $\sim 10^4$ K (Sahu, 1992). However, the temperature at the center region of the Shell has not been estimated, since the line widths are affected by the expansion of the Shell.

The Gum Nebula can be interpreted as an *Ha* shell formed as a result of the interaction of the stars in Vela OB2 with the parent Giant Molecular Cloud and the sorrounding interstellar medium, perhaps even a blister region currently ionized by ζ Puppis and buffeted by stellar winds. OB associations of the order of 10^7 years old have such HII regions around them, with associated neutral hydrogen formed as the bright O stars in the association start evolving away from the main sequence and the ionizing radiation suddenly decreases by a factor of about 10 (Weaver 1978). The HI disk of Reynoso and Dubner (1997) could be such a recombined region. The low levels of extinction towards stars in the nebula (Wallerstein, Silk and Jenkins 1980) suggest that it is *in front of (and probably overlapping with) the IRAS Shell.* Revised distance estimates to the nebula (Franco 1990) are consistent with this view. The scenario for the Gum Nebula that we wish to advance is schematically shown in Fig 2.17. The Gum Nebula is probably neither a classical stellar wind bubble, nor a supershell. Given the recent Hipparcos distances to ζ Puppis and γ^2 Velorum, it is more likely a large blister produced and ionised by these two luminous stars. The spatial association of ζ Puppis with the Vela OB2 association – which is now quite firm thanks to the Hipparcos distance estimates – is still a puzzle! To recall, it is generally believed that ζ Puppis is a fairly young massive star (t $\sim 10^6$ years), while the Vela OB2 association is a much older association. In view of this striking age discrepancy, we wish to regard our suggestion as tentative. But there is no doubt that the

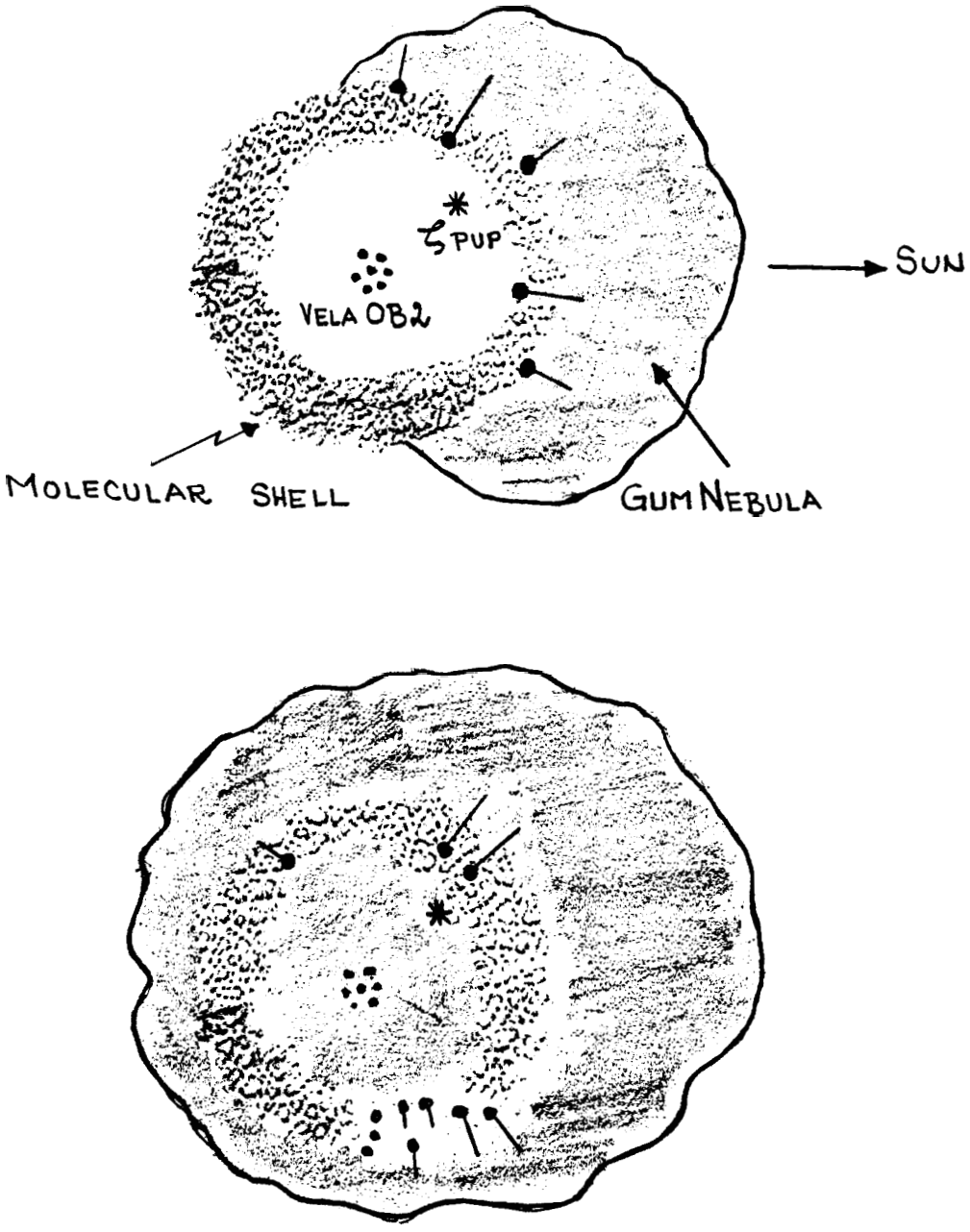

Figure 2.17: Schematic diagrams showing the location of the various important structures in the Gum-Vela region as we conclude from our study of molecular gas in the Shell and recent Hipparcos distances. The bottom figure depicts the view from the Sun.

true nature of ζ Puppis holds the vital clue as to the nature of the Gum Nebula.

2.10.5 Future evolution of the Shell

In the foregoing discussion we stated the case for the IRAS Vela Shell being the expanding remnant of a Giant Molecular Cloud which has been disrupted by the Vela OB2 association. In this section we wish to speculate on the eventual fate of such a shell. As discussed earlier, "super shells", which are giant loops of neutral hydogen have been detected both in our Galaxy and in external galaxies (Heiles, 1979, 1984). A possible origin for such structures is that they are swept up from the interstellar medium by supernovae and stellar winds from OB associations (we refer to McCray, 1988 for a review). There have been extensive modelling of the evolution of such shells (McCray and Kafatos, 1987; McCray and Mac Low, 1988). In these models, *the* the energy input from a series of *supernovae* is *approximated* by a continous energy source, similar to stellar winds. As mentioned in the previous section, the parent Giant Molecular Cloud of the OB association is also likely to be disrupted and swept along. Even after the energy source is exhausted the Shell will continue to plow through the interstellar medium. We shall attempt to relate the future morphology of the molecular shell we have been discussing with those of the well studied "super shells". First we make some simple estimates of the swept-up mass, and other relevant parameters.

The present radius of the Shell is $\sim$ 80 to 90 pc. It is also likely to have a considerable overlap with the Gum Nebula. The density inside the Gum Nebula has a considerable range of values. Reynolds (1976a), using the Ha emission measure and dispersion measure towards pulsars in this direction, estimated the electron density in the Gum Nebula shell to be between 2 and 5 cm^{-3}. Wallerstein, Silk and Jenkins (1980) estimates the electron densities to vary from 0.1 to 100 cm^{-3}. They adopt a mean value for the particle density in the nebula to be 0.3 cm^{-3}. This is the typical density of the intercloud medium, and lends support to our scenario for the Gum Nebula. If the molecular Shell is expanding into such densities, the swept up mass at present would be $\sim 1.5 \times 10^4 M_\odot$. This is a small fraction of the estimated mass in the Shell at present ($\sim 10^5 M_\odot$) and therefore the Shell is likely to be expanding freely. If so, the present expansion age for the Shell is $\sim$ 6.8 x 10^6 years. This is to be compared with the age of the Vela OB2 association which is estimated to be 10^7 years. A more detailed modelling of the Shell would take into account the acceleration of the Shell because of the impulses from supernovae from Vela OB2, and the pressure inside it by conductive

evaporation of the inner region of the Shell by the hot interior. McCray and Kofatos (1987) estimate that the radius of a shell swept up by an OB association would evolve similar to the radius for a stellar wind driven bubble:

$$R_s = 97pc[N_* E_{51}/n_0]^{1/5} t_7^{3/5}$$

where N_* is the number of stars in Vela OB2 likely to explode as supernovae and E_{51} is the energy released per supernova in units of 10^{51} ergs. n_0 is the ambient density, and t_7 is the age in units of 10^7 years. Allowing for such an acceleration would reduce the estimate for the present age of the Shell. Given the present lack of details of the Initial Mass Function of Vela OB2 and the ambient density into which the Shell is expanding, the simple age estimate with free expansion assumed seems justified. As mentioned earlier, the swept up hydrogen should be visible as a neutral shell. We can attempt to arrive at a rough estimate of the column density of the swept up hydrogen in the Shell. We assume a shell thickness of $\sim$ 10 pc, which is $\sim$ 10 % of the radius of the Shell ($\sim$ 90 pc) and is also consistent with the thickness seen in the radiative phase of supershells from the numerical modelling of Mac Low, Norman and McCray (1988). If we further assume that all the estimated swept up mass of $\sim$ 1.5 x 10^4 $M_\odot$ is in this thin Shell, the implied column density in a line of sight along the radius of the Shell is of the order of 2×10^{19} cm^{-2}. This is an overestimate of the column density, since the mass is likely to be distributed over a greater volume. A column density of $\sim 10^{19}$ cm^{-2} in HI is difficult to detect. Moreover one is assuming that the swept up material has cooled to temperatures where the gas is neutral and detectable in line radiation. Following McCray (1988), the cooling time t_c for such swept up shells is given by

$$t_c = 4 \text{ x } 10^6 \text{yr} \zeta^{1.5} [N_* E_{51}]^{0.3} n_0^{-0.7}$$

where N, is the number of stars in the OB association expected to explode as supernovae, E_{51} is the energy of a supernova explosion in units of 10^{51} ergs, n_0 is the density of the ambient medium, and ζ is the metallicity in solar system units. If we assume N, = 24 (Sahu, 1992), $n_0 = 0.3$ cm^{-3}, E_{51} and $\zeta = 1$, this timescale for cooling to temperatures where the radiative loss is important is $\sim 2 \times 10^7$ years. This is to be compared with estimated expansion age of the Shell which is $\sim$ 7 x 10^6 years. Thus most of the swept up mass would not have had enough time to cool to temperatures at which line emission from neutral gas is important. As estimated by McCray (1988), by the time the shells are visible as HI emission features, the parent OB association is unlikely to be existing. Observations so far

have failed to reveal any HI structure coincident with the Shell. Given the above scenario, the sensitivity required and the difficulty of separating out HI emission features in a nearby object given the local gas make this task difficult. **We wish to point out that if indeed the swept up gas is starting to cool through $H\alpha$ radiation from recombinations, it could account for the enhanced Ha emission seen in the Shell.**

As the shell continues to expand and sweep up mass it will decelarate. **When sufficient mass accumulates in the shell it could collapse and secondary cloud formation can occur.** Such secondary cloud formation is one possible explanation for giant star complexes. Star complexes are aggregations of several adjacent and contemporary star clusters extending for hundreds of parsecs in the galactic plane (Efremov 1979). Elmegreen (1982) has pointed out such young clusters and molecular complexes within $\sim$ 200 pc of the double cluster h and χ Persei. **The complex shows evidence of a first generation of clouds which gave rise to h and χ Persei, subsquent disruption of these parent clouds, formation of a giant shell and a second generation of clouds which give rise to the young star forming regions seen around h and χ Persei.**

Another prime example for such secondary cloud and star formation is the Goulds belt. This is a system of O-B stars confined to a plane inclined to the Galactic disc at an angle of $\sim$18° (Gould, 1879). These stars were found to form an expanding system (Bonneau 1964). The study of neutral hydrogen associated with this belt, first carried out by Lindblad et *al.* (1973), revealed an expanding ring of HI associated with the Gould's belt with an expansion age of $\sim$ 60 Myrs (the Lindblad ring). The molecular cloud complexes of Orion, Sco-Cen, Ophiucus, Perseus and the associated star clusters form parts of this giant complex. Fig 2.18, reproduced from Elmegreen (1982) shows the complexes which go to make up the Ring. These molecular clouds are also found to be expanding (Taylor et aZ.1987, Ramesh 1993). The formation of the Gould's belt could have been from a sequence of events similar to the one described for h and χ Persei complex. A first generation star cluster forms at the center of the Belt from a parent cloud. A burst of star formation disrupts the cloud and sweeps out a large cavity and an expanding shell. About 20 Myrs ago this ring probably collapsed to form the Sco-Cen and Orion OB associations and later on the Per OB2 association. The ages of these associations are similar (Blaauw 1964, Stother 1972). Several other giant HI shells also show evidence for molecular clouds along their periphery

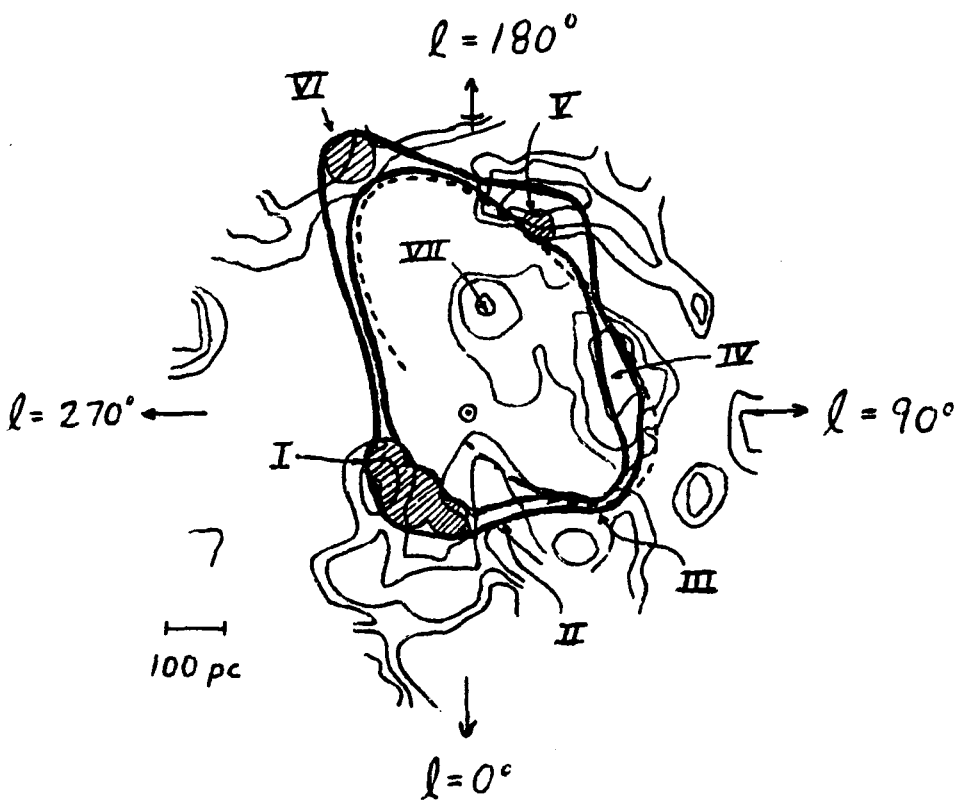

Figure 2.18: A sketch of the various components of the complex of gas, dust and star groups forming the Gould's Belt. The light contours outline dust clouds, the cross hatched circles are OB associations. The dashed ellipse is the model for an expanding HI ring (Lindblad ring). The two heavy lines represent the model for a ring proposed by Elmegreen (1982). The features indicated by Roman numerals are: I - The Sco-Cen OB association; II - Ophiuchus OB association; III - The Great Dark Rift; IV - A large dust cloud; V - Perseus OB association; VI - Orion OB association; VII - Taurus OB association.

(Koo and Heiles, 1988). These are attributed to secondary cloud formation from gravitational or other instabilities in the shells. However, it should be borne in mind that some of the molecular gas seen in the shells are *from the remnant of the parent Giant Molecular Cloud of the OB associations driving the expansion, as seen in the case of the IRAS Shell.*

It is therefore plausible that the future evolution of the IRAS Vela Shell could follow a sequence similar to the one discussed above. Expanding at the present rate (again neglecting acceleration due to interior pressure and subsequent deceleration) the Shell will attain the dimensions of the Goulds Belt ($\sim$ 700 pc) in $\sim 2\times10^7$ years and sweep up $\sim 10^6 M_\odot$. The time estimate does not change much even if one adopts a relation $R_s \propto t_7^{2/5}$ (McCray 1988) for a Shell in the decelerating phase after a time when it has swept up a mass of the order of the Shell mass itself. The estimated swept up mass is of the order of magnitude when instabilities start to set in and collapse is initiated.

2.11 Further work

One of our major aims at the outset was to estimate the mass of molecular material associated with the Shell and compare it with the mass estimates arrived at from IRAS fluxes and assumed dust-to-gas ratios. For this, an estimate of the typical sizes or range of sizes of these gas clouds is to be made. Although there are indications of considerable clumping of the material, as is indicated by the distribution of detections and non detections in Fig 2.5, only a mapping of at least a few of these sources will reveal their sizes. This combined with integrated fluxes in ^{12}CO emission can be used to estimate masses. The mass of the expanding gas is required in any attempt to explain the energetics, nature and possible origins of the IRAS Vela Shell.

References

Allen, C.W. 1973, Astrophysical Quantities (Athlone;London), 3rd ed.

Bally, J., Langer, W.D., Wilson, R.W., Stark, A.A., Pound, M.W. 1990, in IAU Symp. No. 147 on Fragmentation of Molecular Clouds and Star Formation, eds. E.Falgarone, F.Boulanger, G.Duvert., Kluwer, Dordecht.

Bally, J., Scoville, N.Z. 1980, Ap. J., 239, 121.

Bhatt, H.C. 1993, Mon. Not. R. astr. Soc., 262, 812

Blaauw, A. 1961, Bull. Astr. Inst. Netherlands, 15, 265

Blaauw, A. 1964, Ann. Rev. Astr. Ap., 2, 213

Blaauw, A. 1984, in The Birth and Evolution of Massive Stars and Stellar Groups, eds W.Boland and H.van Woerden, D.Reidel, Dordecht, The Netherlands.

Bodenheimer, P., Tenorio-Tagle, G., York, H.W. 1979, Astr. Astrophys., 233, 85.

de Zeeuw, P.T., Brown, A.G.A, de Bruijne, J.H.J, Hoogerwerf, R., Lub, J., Le Poole, R.S., Blaauw, A. 1997, astro-ph/9707089.

Bonneau, M. 1964, J.Obs., 47, 251.

Brand, P.W.J.L., Hawarden, T.G., Longmore, A.J., Williams, P.M., Caldwell, J.A.R. 1983, Mon. Not. R. astr. Soc., 203, 215.

Brandt, J.C., Stecher, T.P., Crawford, D.L., Maran, S.P. 1971, Ap. J.(Letters), 163, L99.

Bruhweiler, F.C., Kafatos, M., Brandt, J.C. 1983, Comments Astrophys. 10, 1.

Chanot, A., Sivan, J.P. 1983, Astr. Astrophys., 121, 19.

Dubner, G., Giacani, E., Cappa de Nicolau, C., Reynoso, E. 1992, Astr. Astrophys. Suppl., 96, 505.

Efremov, Yu.N. 1979, Sov. Astr. Lett., 5, 1.

Elmegreen, B.G. 1982, in Submillimeter wave astronomy, eds. J.E Beckman and J.P. Phillips, Cambridge Univ. Press.

Emerson, J.P. 1987, in Star Forming Regions, ed. M.Piembert & J.Jugaku, D.Riedel Publishing Company., pp 19.

Evans II, N.J., Lada, E.A. 1990, in IAU Symp. No. 147 on F'ragmentation of Molecular Clouds and Star Formation, eds. E.Falgarone, F.Boulanger, G.Duvert., Kluwer, Dordecht.

Feitzinger, J.V., Stuwe, J.A. 1984, Astr. Astrophys. Suppl., 58, 365.

Franco, G.A.P. 1990, Astr. Astrophys., 227, 499.

Garmany, C.D., Stencel, R.E. 1992, Astr. Astrophys. Suppl. 94, 211

Gould, B.A. 1879, Uranometria Argentina (P.E Coni, Buenos Aires) 335.

Gum, C.S. 1952, Observatory 72, 151.
Gum, C.S. 1956, Observatory 76, 150.
Hartley, M., Manchester, R.N., Smith, R.M., Tritton, S.B., Goss, W.M. 1986, Astr. Astrophys. Suppl., 63, 27.
Hawarden, T.G., Brand, P.W.J.L. 1976, Mon. Not. R. astr.. Soc., 175, 19P.
Heiles, C. 1979, Ap. J., 229, 533.
Heiles, C. 1984, Ap. J. Suppl., 55, 585.
Herbst, W. 1975, Astr. J. 80, 503.
Kerr, F.J., Lynden-Bell, D. 1986, Mon. Not. R. astr.. Soc., **221**, 1023.
Koo, B.-C., Heiles, C., 1988, in IAU Coll. No. 101 on Supernova remnants and the Interstellar Medium, eds. R.S Roger and T.L.Landecker, Cambridge Univ. Press.
Leisawitz, D., Bash, F.N., Thaddeus, P. 1989, Ap. J. Suppl., 70, **731**
Lindblad, P.O., Grape, K., Sandqvist, A., Schober, J. 1973, Astr. Astrophys., 24, 309.
Mac Low, M.-M., McCray, R. 1988, Ap. J., 324, 776.
Mac Low, M.-M., Norman, M.L., McCray, R. 1988, in IAU Coll. No. 101 on Supernova remnants and the Interstellar Medium, e d ~R.S Roger and T.L.Landecker, Cambridge Univ. Press.
May, J., Murphy, D.C., Thaddeus, P. 1988, Astr. Astrophys. Suppl. Ser. 73, 51.
McCray, R. 1988, in IAU Coll. No. 101 on Supernova remnants and the Interstellar Medium, eds. R.S Roger and T.L.Landecker, Cambridge Univ. Press.
McCray, R., Kafatos, M. 1987, Ap. J., 317, 190.
Murphy, D.C., Reipurth, B., May, J. 1991, Astr. Astrophys. 247, 202.
Oort, J.H., Spitzer, L. 1955, Ap. J., 121, 6.
Otrupcek, R.E., Hartley, M., Jing-Sheng, W. 199 (private communication, Otrupcek).
Parker, N.D. 1988, Mon. Not. R. astr.. Soc., 235, 139.
Pettersson, B. 1987, Astr. Astrophys., 171, 101.
Prusti, T. 1992, Ph.D. Thesis, University of Groningen.
Ramesh, B. 1993, Ph.D. Thesis, Indian Institute of Science, Bangalore.
Reipurth, B., 1983, Astr. Astrophys., 117, 183.
Reynolds, R.J. 1976a, Ap. J., 203, 151.
Reynolds, R.J. 1976b, Ap. J., 206, 679.
Reynoso, E.M., Dubner, G.M. 1997, Astr. Astrophys. Suppl., 123, 31.
Sahu, M.S. 1992, Ph.D. Thesis, University of Groningen.
Sandqvist, A. 1976, Mon. Not. R. astr. Soc., 177, 69P.

Schaerer, D., Schmutz, W., Grenon, M. 1997, Ap. J.(Letters), 484, L153.
Sivan, J.P. 1974. Astr. Astrophys. Suppl. **16,** 163.
Sridharan, T.K. 1992, Ph.D. Thesis, Indian Institute of Science, Bangalore.
Stothers, R. 1972, Ap. J., 175, 431.
Taylor, D.K., Dickman, R.L., Scoville, N.Z. 1987, Ap. J., 315, 104.
Upton, E.K.L., 1971, in The Gum Nebula and Related Problems, eds. S.P. Maran, J.C. Brandt and T.P Stecher.
van der Hucht, K.A,. Schrijver, H., Stenholm, B., Lundstrom, I., Moffat, A.F.J., Marchenko, S.V., Seggewiss, W., Setia Gunawan, D.Y.A., Sutyanto, W., van den Heuvel, E.P.J, de Cuyper, J.P., Gomez, A.E, 1997, New Astr., 2, 245.
Wallerstein, G., Silk, J., Jenkins, E.B. 1980, Ap. J., 240, 834.
Weaver, R., McCray, C.T., Castor, J., Shapiro, P., Moore, R. 1977, **Ap.** J., 218, 377.
Weaver, T.A., Zimmerman, G.B., Woosley, S.E. 1978, Ap. J., 225, 1021.
Zealey, W.J., Ninkov, Z., Rice, E., Hartley, M., Tritton, S.B. 1983 Astrophys. Lett., 23, 119.

Appendix

In the following set of tables, we present the Galactic co-ordinates, measured velocities (LSR) of the ^{12}CO emission, and projected separation from the assumed center of the Shell of all the objects assumed to be part of the molecular Shell in the Gum-Vela region. These include the molecular material we have detected towards IRAS point sources, the Southern Dark Clouds (SDCs) and the Cometary Globules (CGs).

Source	l^{II}	b^{II}	V_{lsr}	θ	Source	l^{II}	b^{II}	V_{lsr}	θ
	Deg	Deg	km/s	Deg		Deg	Deg	km/s	Deg
51704	251.48	-12.3	-1.2	11.92	60933	267.90	-9.9	0.3	9.64
52594	250.82	-10.8	-2.5	11.50	61322	257.78	-2.7	8.4	2.75
53668	253.22	-10.7	-0.5	9.61	61322	257.78	-2.7	13.2	2.75
53829	253.43	-10.6	-3.4	9.38	61351	260.97	-4.8	8.1	1.10
54473	250.62	-8.4	-1.2	10.43	61428	256.45	-1.6	7.7	4.45
54599	250.88	-8.3	-2.2	10.18	61837	266.33	-7.8	3.0	7.17
54769	255.93	-10.8	-3.1	7.92	62100	259.76	-2.8	9.9	1.28
55878	255.89	-9.3	-5.0	6.74	62578	261.08	-3.0	14.9	1.37
55884	262.22	-12.6	4.4	8.79	62717	267.56	-7.4	3.9	8.09
55925	261.76	-12.3	5.5	8.42	62841	271.22	-9.8	-1.0	12.37
55932	252.47	-7.3	21.5	8.34	62847	264.90	-5.3	5.4	4.88
56549	263.24	-12.3	2.2	8.82	63338	261.81	-2.3	9.4	2.36
56831	253.58	-6.7	-1.5	7.06	63338	261.81	-2.3	14.4	2.36
57035	249.19	-3.8	16.4	10.96	63927	267.91	-6.0	4.6	7.95
57035	249.19	-3.8	28.6	10.96	64029	260.16	0.0	8.8	4.09
57898	264.43	-11.4	1.4	8.50	64154	264.37	-3.0	14.1	4.32
58784	264.69	-10.6	-8.2	7.93	64388	266.94	-4.6	0.9	6.77
58793	256.45	-5.6	8.6	4.04	64728	262.16	-0.4	10.6	4.17
58793	256.45	-5.6	9.6	4.04	64999	270.34	-6.4	-4.0	10.38
59579	265.21	-9.9	-7.5	7.70	65728	263.87	-0.1	7.0	5.39
59584	254.76	-3.4	5.7	5.44	65877	262.26	1.5	4.9	5.90
59891	268.28	-11.4	-6.3	10.88	66001	266.76	-2.0	1.9	6.88
60933	267.90	-9.9	0.3	9.64	67910	269.56	-1.4	6.0	9.74
61322	257.78	-2.7	8.4	2.75	69185	272.15	-1.6	3.5	12.22

Table 2.2: IRAS point sources in the Shell towards which we have detected associated molecular material : Column 1 lists the source number from the IRAS Point Source catalogue; Columns 2 and 3 give the Galactic co-ordinates, Column 4 shows the LSR velocity and Column 5 lists the projected angular separation between the source and the center of the Shell. **The table is continued in Columns 6 to 10 .**

Name	l^{II}	b^{II}	V_{lsr}	θ
	Deg	Deg	km/s	Deg
CG01	256.15	-14.07	3.3	10.80
CG02	255.32	-14.35	4.1	11.39
CG03	260.72	-12.40	0.1	8.36
CG04	259.48	-12.73	1.7	8.71
CG06	258.99	-13.21	0.9	9.24
CG07	266.04	4.31	-1.1	10.21
CG08	255.06	-8.76	-5.8	6.95
CG09	255.06	-9.17	-4.2	7.23
CG10	255.79	-9.18	-5.5	6.75
CG13	259.48	-16.43	3.7	12.40
CG14	262.49	-13.37	-0.9	9.61
CG15	262.88	-14.67	-0.8	10.96
CG16	262.86	-15.48	-0.7	11.74
CG17	270.59	-4.69	3.7	10.43
CG18	269.66	-3.92	2.0	9.49
CG22B1	253.58	2.96	6.5	9.63
CG22B2	253.37	3.24	6.8	9.97
CG24	260.02	-3.82	-12.5	0.27
CG25	260.65	-12.71	-1.8	8.67
CG26	252.15	0.73	2.0	9.34
CG27	251.66	0.15	5.0	9.49
CG28	251.80	0.05	5.2	9.32
CG29	251.88	0.01	5.2	9.23
CG30	253.29	-1.61	5.8	7.30
CG31A	253.19	-1.66	6.0	7.38
CG31B	253.18	-1.72	6.0	7.37
CG31C	253.11	-1.73	6.3	7.44
CG31D	253.11	-1.80	6.9	7.41
CG32A	252.52	0.08	4.9	8.70
CG32B	252.48	0.08	4.8	8.74
CG33	252.29	0.51	1.6	9.11
CG36	256.95	2.65	-8.5	7.43
CG36	256.95	2.65	-8.5	7.43
CG37	251.11	0.52	6.2	10.15
CG38	253.38	-1.64	7.0	7.20

Table 2.3: Cometary Globules: Column 1 lists the Globule number; Columns 2 and 3 give the Galactic co-ordinates, Column 4 shows the LSR velocity and Column 5 shows the projected angular separation between the globule and the center of the Shell.

l^{II}	b^{II}	V_{lsr}	θ	l^{II}	b^{II}	V_{lsr}	θ
Deg	Deg	km/s	Deg	Deg	Deg	km/s	Deg
247.80	-3.2	18.7	12.40	253.40	-4.0	11.8	6.77
249.00	-3.2	17.2	11.20	253.60	-1.3	11.2	7.12
249.00	-3.2	26.2	11.20	253.60	2.9	5.9	9.57
249.40	-5.1	7.2	10.82	253.80	-10.9	-1.3	9.36
249.40	-5.1	18.2	10.82	253.90	-0.6	10.8	7.16
249.70	-2.1	15.6	10.65	253.90	-0.6	35.8	7.16
250.80	-8.1	-1.0	10.21	254.10	-3.6	10.6	6.09
251.10	-1.0	9.6	9.57	254.50	-9.6	-1.7	7.94
251.50	2.0	25.1	10.57	254.70	-1.1	9.8	6.22
251.70	0.2	5.1	9.48	254.70	-1.1	37.1	6.22
251.70	-12.2	-1.3	11.76	255.10	-9.2	-4.6	7.23
251.80	0.0	5.6	9.30	255.10	-8.8	-6.0	6.95
251.90	0.0	5.4	9.21	255.30	-14.4	3.8	11.44
252.10	-3.6	-2.0	8.08	255.30	-4.9	9.8	4.95
252.10	-3.6	7.2	8.08	255.40	-3.9	9.8	4.77
252.10	-3.6	14.5	8.08	255.50	-4.8	10.5	4.73
252.10	-1.3	12.9	8.53	255.60	-2.9	8.9	4.71
252.20	0.7	1.6	9.28	255.80	-9.2	-5.6	6.76
252.30	-3.2	8.5	7.92	255.90	-9.1	-5.4	6.62
252.30	-3.2	12.5	7.92	255.90	-2.6	9.8	4.51
252.50	0.1	4.4	8.72	256.10	-2.1	9.0	4.51
252.90	-1.6	5.9	7.67	256.10	-9.3	-4.3	6.64
252.90	-1.6	11.2	7.67	256.10	-9.2	-4.6	6.57
253.00	-1.7	5.7	7.55	256.10	-9.1	-5.2	6.49
253.00	-1.7	10.3	7.55	256.20	-14.1	3.5	10.81
253.10	-2.1	11.6	7.34	256.40	-10.0	-3.6	7.05
253.10	-1.7	5.4	7.45	256.90	-10.4	-4.5	7.14
253.10	-1.7	9.9	7.45	256.90	-5.4	11.3	3.54
253.20	-4.2	11.8	6.97	256.90	2.6	10.6	7.41
253.30	-1.6	5.2	7.30	257.20	-10.3	-3.7	6.92

Table 2.4: Southern Dark Clouds within 12.5" of the center of the IRAS Vela Shell, from the Mopra Survey (Otrupcek et al., 1995) kindly made available to us by R.Otrupcek.: Column 1 and 2 give the galactic co-ordinates, Column 3 shows the LSR velocity and Column 4 shows the projected angular separation between the source and the center of the Shell. **The table is continued in Columns 5 to 8.**

l^{II}	b^{II}	V_{lsr}	θ	l^{II}	b^{II}	V_{lsr}	θ
Deg	Deg	km/s	Deg	Deg	Deg	km/s	Deg
257.30	-2.5	15.9	3.26	260.40	0.4	6.3	4.46
258.10	-1.9	10.3	2.99	260.40	0.4	9.2	4.46
258.10	-1.9	43.2	2.99	260.40	-8.0	3.4	3.96
258.60	0.3	7.9	4.63	260.40	2.2	7.5	6.25
258.60	0.3	17.3	4.63	260.50	-5.2	5.0	1.20
258.60	-3.4	8.9	1.70	260.60	0.8	5.2	4.87
258.60	-3.4	15.1	1.70	260.60	-3.7	4.5	0.55
258.70	-2.8	10.3	1.93	260.60	-3.7	6.4	0.55
258.90	-4.1	8.5	1.27	260.60	-12.7	-2.4	8.66
259.00	-13.2	4.4	9.23	260.70	-12.4	0.0	8.37
259.00	0.8	5.9	4.99	260.80	0.2	5.8	4.30
259.00	3.6	2.6	7.74	260.80	0.2	8.0	4.30
259.00	3.6	6.4	7.74	260.80	0.2	12.2	4.30
259.10	-4.0	9.5	1.07	261.30	0.2	5.7	4.40
259.10	-3.8	9.5	1.10	261.30	0.2	7.6	4.40
259.20	0.3	4.4	4.46	261.30	0.2	10.9	4.40
259.20	0.3	6.5	4.46	261.50	0.9	6.4	5.12
259.20	0.3	12.3	4.46	261.60	3.0	11.2	7.19
259.20	-13.2	5.2	9.20	261.70	-4.4	8.4	1.57
259.30	0.9	3.6	5.03	261.70	-4.4	11.7	1.57
259.30	0.9	6.7	5.03	261.70	-12.5	6.1	8.59
259.30	0.9	4.5	5.03	262.20	0.4	8.4	4.89
259.40	-12.7	1.1	8.68	262.20	-12.3	4.8	8.50
259.50	-16.4	3.6	12.37	262.20	1.4	4.8	5.81
259.90	-4.4	9.6	0.44	262.40	2.2	6.5	6.63
259.90	0.0	7.9	4.06	262.40	2.2	8.4	6.63
260.00	-3.8	-12.7	0.30	262.50	-13.4	-0.7	9.64
260.10	1.6	5.6	5.65	262.50	-0.4	7.6	4.33
260.10	1.6	6.8	5.65	262.50	-0.4	39.3	4.33
260.20	0.7	5.3	4.75	262.50	2.1	8.4	6.58

Table 2.4: continued from the previous page: Southern Dark Clouds within 12.5" of the assumed center of the IRAS Vela Shell, from the Mopra Survey (Otrupcek et *al.*, 1995): Column 1 and 2 give the galactic co-ordinates, Column 3 shows the LSR velocity and Column 4 shows the projected angular separation between the source and the center of the Shell. **The table is continued in Columns 5 to 8.**

l^{II}	b^{II}	V_{lsr}	0	l^{II}	b^{II}	V_{lsr}	θ
Deg	Deg	km/s	Deg	Deg	Deg	km/s	Deg
262.90	-14.7	-0.5	10.99	265.50	0.0	-6.8	6.69
262.90	2.0	5.0	6.64	265.70	-7.7	3.0	6.62
263.00	1.8	7.1	6.50	265.80	-7.3	3.8	6.50
263.00	1.8	26.9	6.50	265.80	-7.4	3.4	6.55
263.00	1.2	7.8	5.96	266.00	-7.5	3.5	6.77
263.00	-12.0	3.8	8.44	266.00	-4.3	4.9	5.83
263.10	1.8	5.6	6.54	266.10	1.1	2.1	7.85
263.10	1.9	3.8	6.63	266.10	1.1	5.4	7.85
263.20	1.6	5.4	6.41	266.10	1.1	8.4	7.85
263.40	2.0	3.0	6.86	266.10	1.1	12.0	7.85
263.50	1.5	4.8	6.47	266.10	1.1	21.6	7.85
263.50	1.5	8.7	6.47	266.10	-7.7	3.5	6.96
263.70	0.0	5.4	5.37	266.30	-0.7	3.8	6.98
263.70	0.0	9.9	5.37	266.30	-0.7	6.2	6.98
263.90	-3.5	2.8	3.77	266.30	-0.7	10.0	6.98
263.90	-3.5	5.2	3.77	266.40	-0.1	3.8	7.37
264.00	-11.6	4.2	8.47	266.40	-0.1	5.7	7.37
264.30	2.9	11.3	8.08	266.60	5.0	2.5	11.10
264.30	1.5	6.6	6.92	266.90	0.6	5.3	8.18
264.40	5.7	8.9	10.63	267.10	-0.7	1.4	7.70
264.50	5.6	10.0	10.58	267.10	-0.7	6.0	7.70
264.50	5.0	2.5	10.03	267.10	-0.7	18.8	7.70
264.50	-11.3	12.0	8.44	267.20	-7.2	4.9	7.70
265.20	-0.6	5.7	6.10	267.20	0.0	4.5	8.11
265.30	0.0	6.5	6.53	267.20	0.0	6.7	8.11
265.30	5.3	3.0	10.66	267.20	0.0	8.8	8.11
265.30	0.6	4.7	6.92	267.40	-0.9	4.0	7.88
265.30	0.6	6.7	6.92	267.40	-0.9	6.6	7.88
265.40	0.2	6.0	6.74	267.40	-0.9	8.3	7.88
265.40	0.2	7.7	6.74	267.40	-7.5	8.6	8.01

Table 2.4: continued from the previous page: Southern Dark Clouds within 12.5" of the assumed center of the IRAS Vela Shell, from the Mopra Survey (Otrupcek *et* al., 1995): Column 1 and 2 give the galactic co-ordinates, Column 3 shows the LSR velocity and Column 4 shows the projected angular separation between the source and the center of the Shell. **The table is continued in Columns 5 to 8.**

l^{II}	b^{II}	V_{lsr}	θ	l^{II}	b^{II}	V_{lsr}	θ
Deg	Deg	km/s	Deg	Deg	Deg	km/s	Deg
267.50	-7.4	5.8	8.06	269.40	3.0	-1.4	11.61
267.60	-6.4	5.8	7.79	269.50	-7.6	4.8	9.98
267.60	-6.0	5.6	7.68	269.50	4.0	-3.8	12.32
267.60	4.3	1.3	11.18	269.70	-3.9	2.2	9.53
267.60	-7.4	5.6	8.15	269.90	-11.1	-0.5	12.01
267.70	-7.4	5.7	8.24	269.90	-11.1	0.8	12.01
267.90	0.6	0.1	9.02	269.90	1.8	-3.0	11.35
267.90	0.6	2.7	9.02	269.90	1.8	4.2	11.35
267.90	3.6	0.5	10.87	270.20	-1.0	1.8	10.48
267.90	3.6	2.1	10.87	270.20	-1.0	7.2	10.48
267.90	-7.8	6.7	8.59	270.20	-1.0	9.6	10.48
268.00	1.8	-5.4	9.77	270.30	2.9	-4.2	12.28
268.00	1.8	-0.6	9.77	270.60	-4.7	3.5	10.45
268.10	-9.5	6.1	9.62	270.70	0.5	-0.2	11.47
268.20	-9.7	5.9	9.82	270.70	0.5	6.2	11.47
268.20	-8.9	4.8	9.38	270.80	-8.5	-0.6	11.52
268.20	-9.5	5.5	9.70	270.80	-8.5	0.8	11.52
268.20	-2.7	7.5	8.14	270.90	-1.6	5.6	11.00
268.20	-2.7	14.4	8.14	271.80	-1.3	-3.9	11.95
268.30	-3.2	1.1	8.17	271.80	-1.3	-1.4	11.95
268.30	-1.9	3.1	8.41	271.80	-1.3	2.7	11.95
268.40	-1.2	4.7	8.71	272.00	-0.2	-0.8	12.44
268.90	0.3	0.7	9.75	272.00	-0.2	4.8	12.44
268.90	0.3	4.8	9.75	272.10	-3.4	8.2	11.95
268.90	0.3	8.4	9.75	272.50	-3.9	4.8	12.33
268.90	-1.2	4.7	9.18	272.50	-3.9	6.2	12.33
269.10	-1.3	2.6	9.34				
269.10	-1.3	6.0	9.34				
269.10	-1.3	7.7	9.34				
269.10	-1.3	9.1	9.34				

Table **2.4:** continued from the previous page: Southern Dark Clouds within **12.5**" of the assumed center of the IRAS Vela Shell, from the Mopra Survey (Otrupcek et al., **1995):** Column **1** and **2** give the galactic co-ordinates, Column **3** shows the LSR velocity and Column **4** shows the projected angular separation between the source and the center of the Shell. **The table is continued in columns 5 *to* 8.**